Palaeogeography, Palaeoclimatology, Palaeoecology 700 (2026) 114095

Contents lists available at ScienceDirect

Palaeogeography, Palaeoclimatology, Palaeoecology

journal homepage: www.elsevier.com/locate/palaeo

Against all odds: The survival of *Porites* corals through the Mediterranean Messinian Salinity Crisis☆

Juan C. Braga[a,*], Alessandro Vescogni[b], Fernando Sola[c], Francesca R. Bosellini[b], Julio Aguirre[a]

[a] *Departamento de Estratigrafía y Paleontología, Universidad de Granada, Granada, Spain*
[b] *Dipartimento di Scienze Chimiche e Geologiche, Università di Modena e Reggio Emilia, Via Campi 103, 41125 Modena, Italy*
[c] *Departamento de Biología y Geología, Universidad de Almería, Almería, Spain*

ARTICLE INFO

Editor: L Angiolini

Keywords:
Post-evaporitic corals
Terminal carbonate complex
Sorbas Basin
Salento Peninsula
SE Spain
SE Italy

ABSTRACT

Despite many reports on the occurrence of reef corals in post-evaporitic Messinian deposits, it is generally assumed that coral reefs disappeared from the Mediterranean region during the Messinian Salinity Crisis. Contradicting this supposition, here we describe coral buildups and associated fossil assemblages that occur in the so-called Terminal Carbonate Complex (TCC) in the Sorbas Basin and Cabo de Gata in SE Spain, and in the Salento Peninsula in SE Italy. In the Sorbas Basin, the TCC conformably overlies the Messinian gypsum and onlaps the basin margins covering an erosion surface on top of pre-evaporitic Messinian coral reefs. This unit is late Messinian in age according to both its planktonic foraminifer assemblages and chronostratigraphic constraints in underlying and overlying units. A late Messinian age has also been proposed for the TCC in Cabo de Gata and Salento. The buildups are constructed by the zooxanthellate coral *Porites,* with minor *Siderastrea* in Salento. They formed structures metres to tens of metres wide and decimetres to a few metres high surrounded by bioclastic to oolitic detrital carbonate locally mixed with siliciclastics. Isolated *Porites* colonies, echinoids, diverse molluscs, coralline and dasycladalean algae occur associated with the buildups in the TCC deposits, in which microbial carbonate domes are also common. The occurrence of coral buildups in the western and central Mediterranean indicates that it is not a local phenomenon but the record of normal marine waters in the post-evaporitic Messinian and the widespread survival of reef corals in the Mediterranean in the late Messinian.

1. Introduction

The nature and timing of paleoenvironmental events in the Mediterranean region during the Messinian Salinity Crisis (MSC) have been under continuous debate ever since the discovery of evaporites in the deep Mediterranean sedimentary pile (Hsü, 1972; Hsü et al., 1973). Most proposed models for the Mediterranean evolution during the Messinian assume that no coral reefs occur in the region postdating the evaporites (e.g. Agiadi et al., 2024a, 2024b). Some papers, however, reported decades ago the occurrence of *Porites* patch reefs in a clearly post-evaporitic unit in the Sorbas Basin (Riding et al., 1991a, 1998; Martín et al., 1993; Braga et al., 1995, 2006) as well as in other localities in SE Spain, within the so-called Terminal Carbonate Complex (hereafter TCC, Esteban, 1979), a sedimentary unit traditionally correlated with the post-evaporitic unit in the Sorbas Basin (Esteban, 1979; Esteban and Giner, 1980; Riding et al., 1991a; Franseen and Mankiewicz, 1991; Franseen et al., 1993; Calvet et al., 1996; Goldstein et al., 2013; Lipinski et al., 2013). Bosellini et al. (1999) and Vescogni et al. (2022, 2025) also reported the occurrence of *Porites* buildups in the NF3 sequence of the Novaglie Formation in the Salento Peninsula in southern Italy, which is late Messinian in age and can be correlated with the TCC in SE Spain (Vescogni et al., 2022). Aggrading *Porites* reefs also occur within the TCC in the Melilla–Nador Basin (Morocco) (Saint Martin et al., 1997; Cunningham et al., 1997; Garcia et al., 2004; Cornée et al., 2006). *Porites*–microbial buildups have been described in the Castelvetrano Basin (western Sicily) within a sedimentary unit potentially attributable to the TCC (Saint Martin et al., 1996). In several other Mediterranean localities, carbonate deposits with diverse lithofacies, but lacking in situ coral buildups, have been correlated with the TCC (i.e. Mallorca, Esteban, 1979; Pomar et al., 1996; Mas and Fornós, 2012; Sardinia,

☆ This article is part of a Special issue entitled: 'Mediterranean Miocene' published in Palaeogeography, Palaeoclimatology, Palaeoecology.

* Corresponding author.
E-mail address: jbraga@ugr.es (J.C. Braga).

https://doi.org/10.1016/j.palaeo.2026.114095
Received 19 December 2025; Received in revised form 21 July 2026; Accepted 21 July 2026
Available online 29 July 2026

Cornée et al., 2008; Malta, Saint Martin et al., 1997; Lampedusa, André et al., 2002).

Although works focused on paleobiogeography and environmental significance of zooxanthellate corals in the Mediterranean Miocene acknowledge the occurrence of upper Messinian patch reefs in the Almería basins (Bosellini and Perrin, 2008; Perrin and Bosellini, 2012, 2013; Vertino et al., 2014), the majority of publications dealing with the Mediterranean Basin evolution during the Messinian ignored the records of post-evaporitic coral reefs in the Betic basins and their obvious implication for the existence of at least a marine episode during the late Messinian in the Mediterranean Basin (Krijgsman et al., 1999, 2001; Rouchy and Caruso, 2006; CIESM (Comm. Int. Explor. Sci. Méditerr.), 2008; Roveri et al., 2014, 2025; Garcia-Castellanos et al., 2025). Even works specifically dealing with the post-evaporitic units of the Sorbas and Cabo de Gata areas ignored the occurrence of coral buildups and attributed the wealth of previous reports to misinterpretations of blocks derived from the underlying lower Messinian reefs as in situ corals (Bourillot et al., 2010a, 2010b, 2020; Clauzon et al., 2015).

Here, we revisit localities in the Sorbas Basin and the Cabo de Gata volcanic province (La Molata, La Rellana and Mesa de Roldán) in SE Spain (Fig. 1A), in which the occurrence of post-evaporitic buildups of zooxanthellate corals has been reported. Except in the case of Mesa de Roldán, no details on the geometry, structure and composition of those buildups were included in the previous reports, focused on other aspects of the geology of the Messinian deposits. We also examine in detail the upper Messinian buildups in the Leuca area of the Salento Peninsula in southeastern Italy (Fig. 1A), which demonstrate that the growth of post-evaporitic zooxanthellate corals also occurred in the central Mediterranean and was not restricted to the Betic basins.

Fig. 1. A. Study areas (red stars) with post-evaporitic Messinian coral buildups in the western and central Mediterranean region (Almería, SE Spain, and Salento, SE Italy). B. Neogene sedimentary basins in Almería (SE Spain) and location of maps in Figs. 2 and 4 (red insets) (taken from Martín et al., 2003). (For interpretation of the references to colour in this figure legend, the reader is referred to the web version of this article.)

The aims of this paper are 1) to describe and illustrate the coral buildups in a sedimentary unit physically overlying the evaporites in the Sorbas Basin in SE Spain, which is biostratigraphically constrained to the late Messinian, and in other units in SE Spain and in the Salento Peninsula in SE Italy, which have been dated as late Messinian by different methods; 2) to interpret the palaeoenvironments in which those reefs grew; and 3) to try to frame their occurrence in the complex events of the Mediterranean evolution during the Messinian.

2. Geological settings

The examined post-evaporitic corals occur in separate localities in two areas in SE Spain and in the Salento Peninsula, whose geological settings and Messinian successions are different although showing certain similarities.

2.1. Sorbas Basin

The Sorbas Basin is an east-west trending synform depression within the Internal Zones of the Betic Cordillera (Figs. 1B and 2). Basin sediments range in age from Middle Miocene to Quaternary. The Messinian succession (Fig. 3A) begins with mixed terrigenous-bioclastic heterozoan carbonates (Azagador Member), which grade upwards and laterally into marls (lower Abad Member) late Tortonian-earliest Messinian in age (Sierro et al., 1993; Sánchez-Almazo et al., 2001). A minor erosion surface separates the heterozoan carbonates from the overlying lower Messinian reef units: Bioherm Unit, *Halimeda* and coral bioherms (Braga et al., 1996; Martín et al., 1997); and Fringing Reef Unit, prograding coral reefs (Riding et al., 1991a; Braga and Martín, 1996). Both units pass laterally into marls (upper Abad Member) early Messinian in age (Sierro et al., 1993, 2001; Krijgsman et al., 1999). An erosion surface separates the reefs and the laterally equivalent pelagic marls from the overlying sediments. In the basin center, the topography of the erosion surface is filled by gypsum beds alternating with fine-grained siliciclastic beds (Yesares Member), which onlap the surface towards the margins (Martín and Braga, 1994; Riding et al., 1998). The gypsum and the reefs at the basin margin are overlain by the Sorbas Member that mainly consists of sandstones, siltstones and marls, and its laterally equivalent TCC that is the subject of this study (see below) (Figs. 2, 3A, B), which transitions upwards to continental deposits (Zorreras Member). An erosion surface carved in the latter materials is covered by a thin package of marine sandstones, early Zanclean in age (Roveri et al., 2019). The infill of the basin ended with continental conglomerates and sandstones (Góchar Member, Mather, 1991) with a top basin surface dated as Early Pleistocene (Stokes et al., 2018).

2.1.1. The post-evaporitic unit with coral buildups

The evaporites in the basin centre (Yesares Member) gradually transition upward to sandstones and siltstones with interbedded silty marls, the Sorbas Member of Ruegg (1964). Northward, these fine-grained deposits pass upslope into coarse fan-delta sediments (the Terminal Complex of Martín et al., 1993), which onlap the underlying, eroded, lower Messinian fringing reefs (Fig. 3B). These deposits are equivalent to the TCC (Esteban, 1979) but were identified with the broader name Terminal Complex because of the abundant siliciclastic sediments in this area. However, to simplify the terminology here we will refer to it as TCC as well. They are siliciclastic conglomerates and sandstones with oolites, *Porites* buildups and abundant microbial carbonates. Carbonates in this sequence, like most of those of Messinian age in the region, are locally dolomitised.

The post-evaporitic reef unit overlies the Yesares Member gypsum, which in turn unconformably overlies pelagic marls, the top of which, below the erosion surface that separates them from the gypsum, has been dated at 5.96 Ma (Krijgsman et al., 1999) in the basin centre and at 5.89 Ma (Sanchez-Almazo et al., 2007; Cuevas-Castell et al., 2007; Rodríguez-Tovar et al., 2013) or 5.87 Ma (Reolid et al., 2016) at the

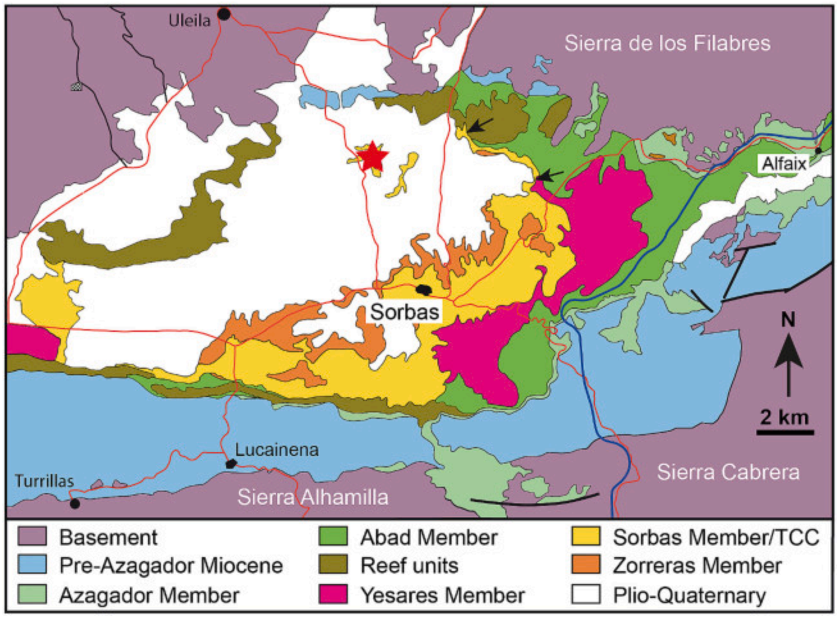

Fig. 2. Geological map of the Sorbas basin with location of the Rambla de Góchar outcrop (red star) (after Montenat, 1990). Note the lateral continuity of the Sorbas Member/TCC from the top of the lower Messinian reefs to the top of the Yesares Member gypsum (arrows). (For interpretation of the references to colour in this figure legend, the reader is referred to the web version of this article.)

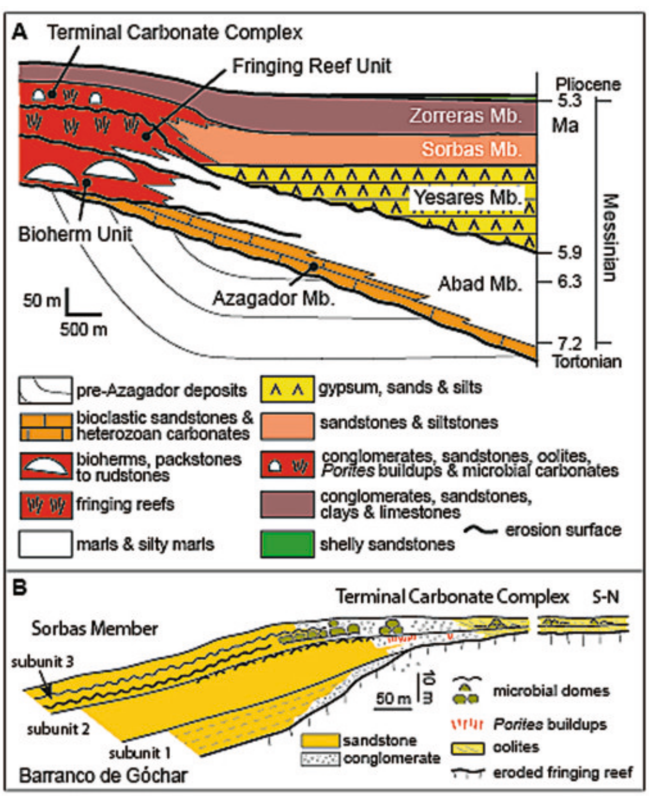

Fig. 3. A. Messinian to Early Pliocene stratigraphy of the Sorbas Basin (modified from Martín and Braga, 1994). B. Section of the basinal Sorbas Member (orange) and marginal equivalent Terminal Carbonate Complex in the Barranco de Góchar outcrop.

northern basin margin. The silty marls in the Sorbas Member/TCC yielded a planktonic foraminifer assemblage comprising *Globigerina multiloba* Romeo, 1965, *Globigerina* sp., *Globoturborotalita* cf. *decoraperta* (Takayanagi and Saito, 1962), *Globigerinoides obliquus* Bolli 1957, *Trilobatus sacculifer* (Brady, 1877), *T. trilobus* (Reuss, 1850), *Orbulina universa* d'Orbigny, 1839, *Neogloboquadrina acostaensis* (Blow, 1959), *N. humerosa* (Takayanagi and Saito, 1962), *Globigerinella pseudobesa* (Salvatorini, 1967), *Globorotalia scitula* (Brady, 1882), *Globoconella miotumida* (Walters, 1965) in a section at the kilometre 497.4 of the road N-340a (Riding et al., 1998). Sánchez-Almazo (1999) reports *Globigerina multiloba*, *Gg.* cf., *bulloides* d'Orbigny, 1826, *Gg. falconensis* Blow, 1959, *Orbulina universa*, *Globoturborotalita* cf. *decoraperta*, *Globoconella miotumida*, *Globorotalia scitula*, *Neogloboquadrina acostaensis* from samples in the section of Cortijo del Hoyo. The Sorbas Member/TCC changes upwards to the fluviatile-lacustrine deposits of the Zorreras Member, which are unconformably overlain by marine sandstones dated as earliest Zanclean within the MNN12a biozone by Roveri et al. (2019). In summary, the post-evaporitic reef unit is late Messinian in age.

2.2. Cabo de Gata area

The Cabo de Gata area is a volcanic province separated from the rest of the Betic Cordillera by the sinistral strike-slip Carboneras fault system (Fig. 1B and 4). In this area, Miocene deposits, mainly carbonates, appear intercalated with and overlying volcanic rocks. Upper Messinian coral buildups occur associated with ooid grainstones and microbial carbonates in units attributed to the TCC in several localities. The TCC overlies an erosion surface on top of lower Messinian reefs (Esteban and Giner, 1980; Riding et al., 1991a; Franseen and Mankiewicz, 1991; Franseen et al., 1993, 1997; Goldstein et al., 2013). We examined the coral buildups in the three following localities.

2.2.1. La Molata

The Messinian succession begins with heterozoan carbonates (Fig. 5). These carbonates are unconformably overlain by lower Messinian reefs, comprising a lower unit of coral patches and bioherms (Martín et al., 2003; Bourillot et al., 2009) and an upper reef unit of prograding clinobeds with reef framework in the upper parts and debris fining downslope (Franseen and Mankiewicz, 1991; Franseen et al., 1993, 1997; Martín et al., 2003). The TCC overlies an erosion surface and is the last outcropping unit. According to Franseen et al. (1998) the age of the TCC in La Molata is approximately 5.8–5.3 Ma, i.e. late Messinian, and, therefore, is partially or totally equivalent to the

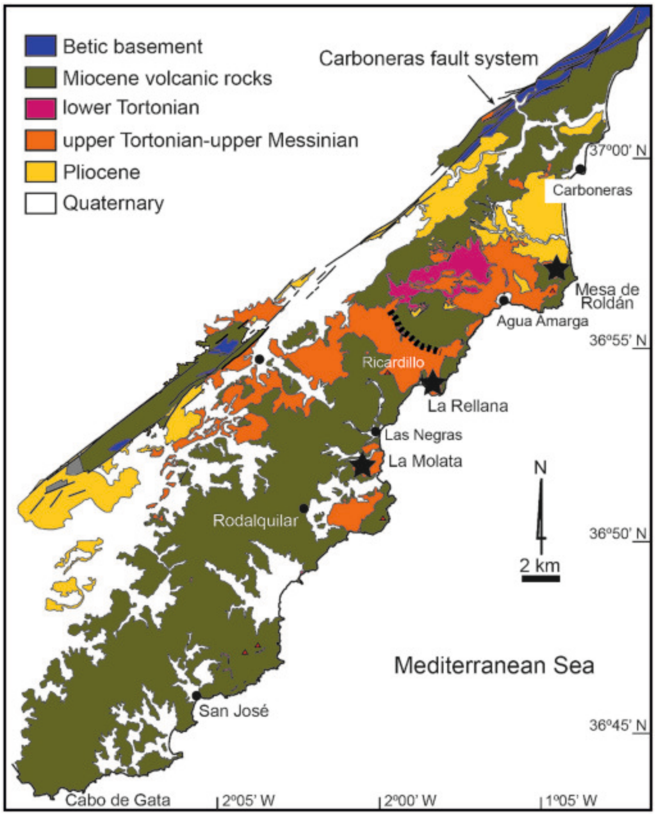

Fig. 4. Geological map of the Cabo de Gata volcanic province with location of the La Molata, La Rellana and Mesa de Roldán outcrops (black stars) (after Martín et al., 2003). The sinistral strike-slip Carboneras fault system separates the Cabo de Gata province from the rest of the Betic Cordillera.

biostratigraphically dated TCC in the Sorbas Basin.

2.2.2. La Rellana

Heterozoan carbonates, which grade laterally and upwards into finer-grained basinal sediments, are late Tortonian-early Messinian in age (Martín et al., 1996). These heterozoan carbonates, equivalent to the Azagador Member in the Sorbas Basin, overlie volcanic and volcanoclastic rocks and are followed by lower Messinian reefs (Betzler et al., 2000; Brachert et al., 2001; Goldstein et al., 2013). As in La Molata, the TCC occurs on an erosion surface at the top of the hill and is assumed to have the same age.

2.2.3. Mesa de Roldán

The study section crops out on an isolated hill on the northern side of the Mesa de Roldán, 6 km south of Carboneras. The Miocene sediments overlie a volcanic dome 8.25 ± 0.07 Myr old (Mattei et al., 2014). The succession comprises lower Messinian reefs (Esteban and Giner, 1980; Brachert et al., 2001, 2002) followed by a small outcrop of TCC at the top of the hill (Riding et al., 1991a).

2.3. Salento Peninsula

The coral buildup examined in this study is exposed a few hundred metres north-west of Punta Ristola, along the present-day coastline (39°47′34.916"N, 18°20′33.014″E) (Figs. 6A, 7).

In the study area (Fig. 6A), the sedimentary succession consists of a series of carbonate depositional sequences, stacked one upon the other and typically separated by significant hiatuses caused by non-depositional or erosional phases (Fig. 6B, C) (Bosellini et al., 1999). The oldest outcropping unit is the Altamura Limestone Formation, composed of Campanian–Maastrichtian shallow-water deposits (Bosellini and Parente, 1994; Bosellini et al., 1999). The Altamura Limestone is overlain by the Castro Limestone Formation, a well-developed lower Chattian coral reef, which is represented in this zone by bioclastic slope deposits (Bosellini et al., 2021 and references therein). A major phase of tectonic subsidence during the Serravallian–Tortonian, coupled with nutrient-rich currents from the eastern Mediterranean, led to the deposition of a thin phosphatic hardground, known as the *Aturia* level, which capped the entire area corresponding to the present-day southeastern Salento (Föllmi et al., 2015; Vescogni et al., 2018). The restoration of shallow-water conditions during the Messinian led to the development of a series of distinct carbonate units, influenced by various depositional environments and changing environmental conditions over time (Bosellini et al., 2001, 2002; Bossio et al., 2002; Bosellini, 2006; Brachert et al., 2007; Vescogni et al., 2008, 2011; Braga et al., 2009; Passaseo and Morsilli, 2024). These deposits mainly belong to the Novaglie Formation (Fig. 6c), which consists of three superimposed sequences that border the south-eastern margin of the Salento platform. The two lower sequences (NF1 and NF2) are lower Messinian *Porites* coral reefs, up to 120 m and 20 m thick, respectively, and represent bioconstructed margins associated with slope deposits. Landward, NF1 and NF2 turn into back-reef oolitic and bioclastic deposits, which belong to the Andrano Calcarenites Formation. The third Novaglie Formation sequence (NF3) consists of up to 12 m of microbialites, oolites, and sparse *Porites* colonisations (Bosellini et al., 1999; Vescogni et al., 2022, 2025), the latter being the focus of the present study. NF3 has recently been dated to the late Messinian through $^{87}Sr/^{86}Sr$ isotopes analyses (Vescogni et al., 2022). Based on its similarity in composition and age to the western Mediterranean TCC (Riding et al., 1991a; Martín et al., 1993; Braga et al., 1995), the NF3 has been named Salento Peninsula TCC (SP-TCC) (Vescogni et al., 2022). The Messinian deposition ended with the Leuca Breccia Formation, a 12 m thick breccia deposit derived from the erosion of the underlying NF3. More recent sediments in the Leuca area are represented by scattered outcrops of middle Zanclean marls and by the Uggiano la Chiesa Formation, several metres thick breccia and calcarenite deposits dating to the Piacenzian–Gelasian (Bosellini et al., 1999).

3. Materials and methods

Data on stratigraphic setting, sedimentary and palaeontological features at the macroscopic scale of post-evaporitic coral buildups were collected in the field. Special attention has been given to the coral colonies, with descriptions of their size, shape, growth form and their taxonomic classification at genus level. Eighteen thin sections (6 × 4.5 cm) were prepared from 12 samples for microfacies analysis of both the coral buildup and the associated sediment in the Salento Peninsula. Thirty-one smaller thin sections (4.5 × 2.5 cm) were used to observe the petrography and components of the Almería buildups. Carbonate textures were classified according to Dunham (1962) terminology with the modifications proposed by Embry and Klovan (1971). Coralline algal nomenclature follows AlgaeBase (Guiry and Guiry, 2025).

4. Results

The following sections describe the corals and associated buildups in post-evaporitic deposits in the investigated areas.

4.1. Post-evaporitic buildups in the Sorbas Basin

4.1.1. The Rambla de Góchar outcrop

According to Martín et al. (1993) at the Rambla de Góchar locality, where the coral buildups are best exposed, three depositional subunits can be distinguished (Fig. 3B). Subunit 1 consists of conglomerates and sandstones up to 25 m thick accumulated on the erosion surface carved on the older fringing-reef slope. Subunit 2 includes conglomerates and sandstones up to 30 m thick that lap onto the truncated reef and extend

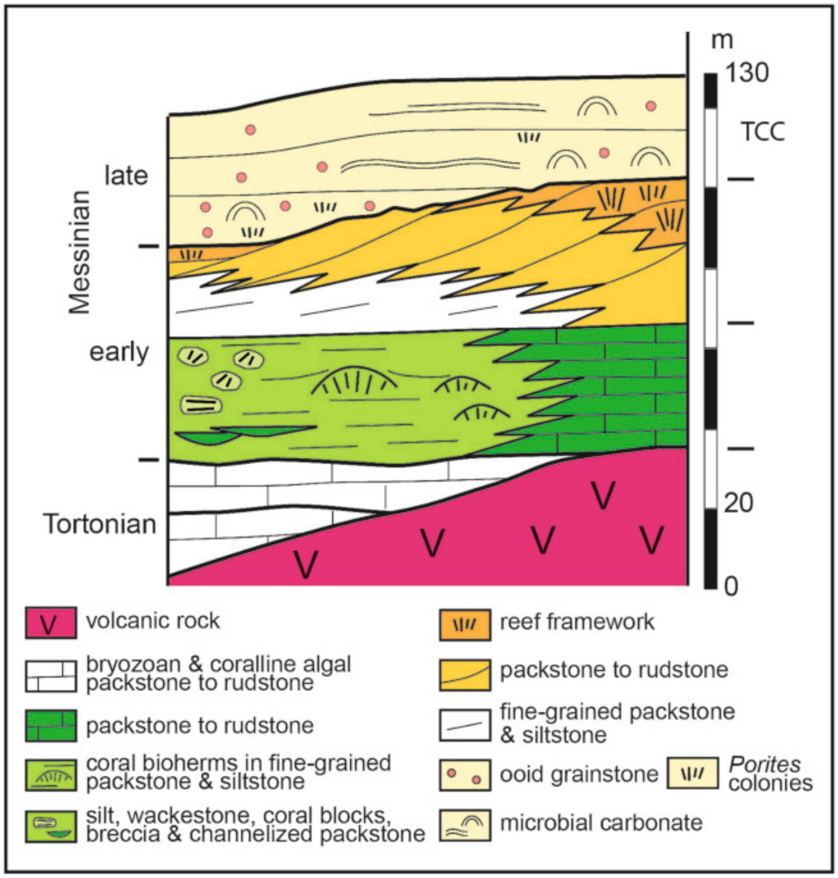

Fig. 5. Stratigraphic scheme of La Molata (after Martín et al., 2003). The Miocene stratigraphy in La Rellana is similar except for a higher volcanoclastic content in the lower Tortonian unit.

over the shelf on top of it. *Porites* buildups occur in this unit intercalated with conglomerates, sandstones and stromatolite domes (see below). Subunit 3 comprises conglomerates and sandstones up to 15 m thick with two stromatolite and thrombolite beds which extend downslope from the shelf-edge for more than 300 m. Shoreward, the shelf deposits of subunits 2 and 3 include ooid grainstones and sandstones with abundant ripples and cross laminations. Locally oolite stromatolite-thrombolite domes occur among the ooid grainstones. These domes are similar to those described from the Níjar area by Riding et al. (1991b) and from La Molata and La Rellana de San Pedro by Goldstein et al. (2013) and Lipinski et al. (2013).

At the logged section (Fig. 8A), overlying the erosion surface, the lower 4.6 m of the TCC consist of three clast- to matrix-supported conglomerate beds with channelised bases (Fig. 8B). The clasts are highly heterometric quartzites and micaschists, up to 60 cm in size, from the Nevado-Filabride complex, the basement to the north, and bioclasts, including molluscs, echinoids, serpulids, encrusting foraminifera and coralline algae (*Spongites* sp. and *Lithophyllum* sp.). The matrix is a muddy sandstone rich in bioclasts. These conglomerates are overlain by greenish medium sandstones, 1.6 m thick, which in turn are covered by a matrix-supported conglomerate, up to 0.7 m thick, with channelised base. It is made of heterometric clasts, up to 30 cm in size, of quartzite, micaschists, and limestones from older Miocene deposits in a sandy matrix. The lower coral buildup settled on this conglomerate. It is a lens-shaped structure up to 2.2 m high and about 25 m wide (Fig. 8A). It is built by branching-columnar *Porites* colonies (Fig. 8C, E) mixed with laminar contorted *Porites* colonies (Fig. 8C, D), grouped in clusters separated by mixed siliciclastic-bioclastic sediment. Some coral colonies are tilted down but the majority appear in growth position (Fig. 8C, D, E). Branching-columnar colonies are less than 1 m high and several decimetres wide. Individual columns are 2–4 cm in diameter and are joined by laminar bridges less than 1 cm thick (Fig. 8E). Laminar contorted colonies are several decimetres high. Individual laminae, 1–3 cm thick, are linked by finger-like projections 10–15 cm high. The coral skeletons were partially lined by encrusting foraminifers and coralline algae (*Lithophyllum* sp. and?*Spongites* sp.) and encrusted with microbial carbonate. The remaining voids in the framework were partially filled with internal sediment, including echinoids and fragments of molluscs and coralline algae. The corals are extensively dissolved and preserved as voids in the microbialite framework (Fig. 8D, E). The buildup was buried by a channelised clast-supported pebble conglomerate, 1.6 m in maximum thickness, composed of clasts of quartzite, micaschists, and Miocene limestones in a sandy matrix. The conglomerate is overlain by 2.6 m of laminated sandstones with bioclasts and superficial ooids, which at the base intercalate a body of thrombolitic domes rich in trapped grains, mostly ooids, 0.8 m high and 2 m wide. The succession continues with a laterally discontinuous bioclastic breccia, 30–40 cm thick, with molluscs and *Porites* fragments and quartzite grains in a wackestone to packstone matrix. *Ostrea, Pseudochama, Barbatia*, venerids, cardiids, and limids can be identified among the moulds remaining after dissolution of the aragonitic shells. The breccia is the base of the upper coral buildup (Fig. 8A), 3.2 m in maximum thickness and about 33 m in lateral extension. *Porites* is the only reef-building coral, and the internal structure, coral morphologies and composition of the framework are like those of the lower buildup (Fig. 8F, G). The succession ends with sandy packstones to rudstones, 3.5 m in thickness, which intercalate microbial carbonate domes very rich in trapped grains, up to 1.4 m high.

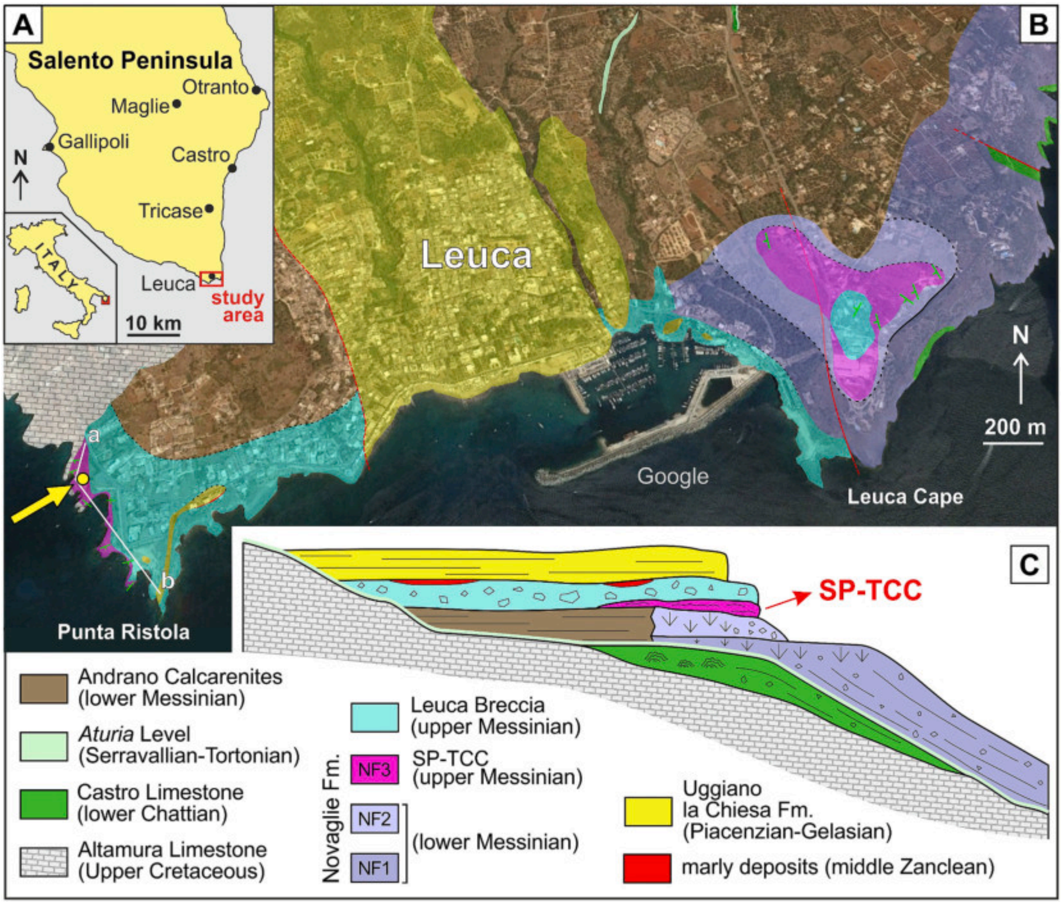

Fig. 6. A. Schematic map of the Salento Peninsula showing the location of the study area. B. Geological map of the study area with the trace of the transects illustrating the SP-TCC architecture at Punta Ristola, as shown in Fig. 7. The yellow arrow marks the position of the investigated *Porites* buildup (modified from Vescogni et al., 2022). C. Stratigraphic framework of the study area; the arrow indicates the stratigraphic unit analyzed in this study, referred to as the SP-TCC (Salento Peninsula Terminal Carbonate Complex). (For interpretation of the references to colour in this figure legend, the reader is referred to the web version of this article.)

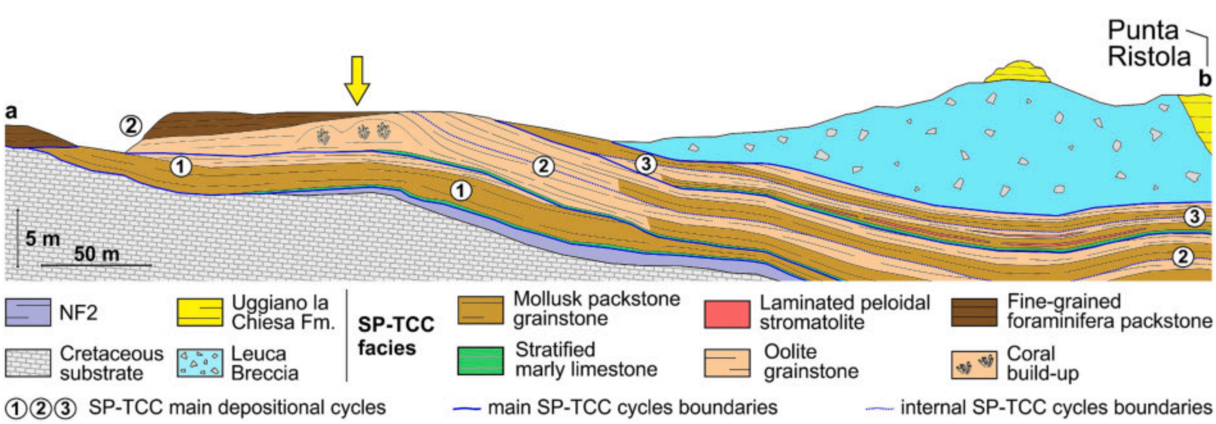

Fig. 7. SP-TCC stratigraphic setting and depositional facies at Punta Ristola (transect a–b in Fig. 6B). The yellow arrow indicates the position of the investigated *Porites* buildup (modified from Vescogni et al., 2022). (For interpretation of the references to colour in this figure legend, the reader is referred to the web version of this article.)

4.2. Post-evaporitic coral buildups in Cabo de Gata

4.2.1. La Molata

The TCC occurs at the top of the La Molata hill overlying a subaerial exposure surface (Figs. 5, 9A) (Franseen and Goldstein, 1996; Martín et al., 2003; Bourillot et al., 2010a; Goldstein et al., 2013; Lipinski et al., 2013). Bourillot et al. (2010a), Goldstein et al. (2013) and Lipinski et al. (2013) interpreted this surface as the local record of the drawdown of the Mediterranean Sea during the MSC, considering this subaerial surface as the time equivalent to the Lower Evaporite in the Mediterranean. According to Franseen et al. (1998) the age of the TCC in La Molata is approximately 5.8–5.3 Ma, i.e. late Messinian, and, therefore, is partially or totally equivalent to the biostratigraphically dated TCC in the Sorbas Basin.

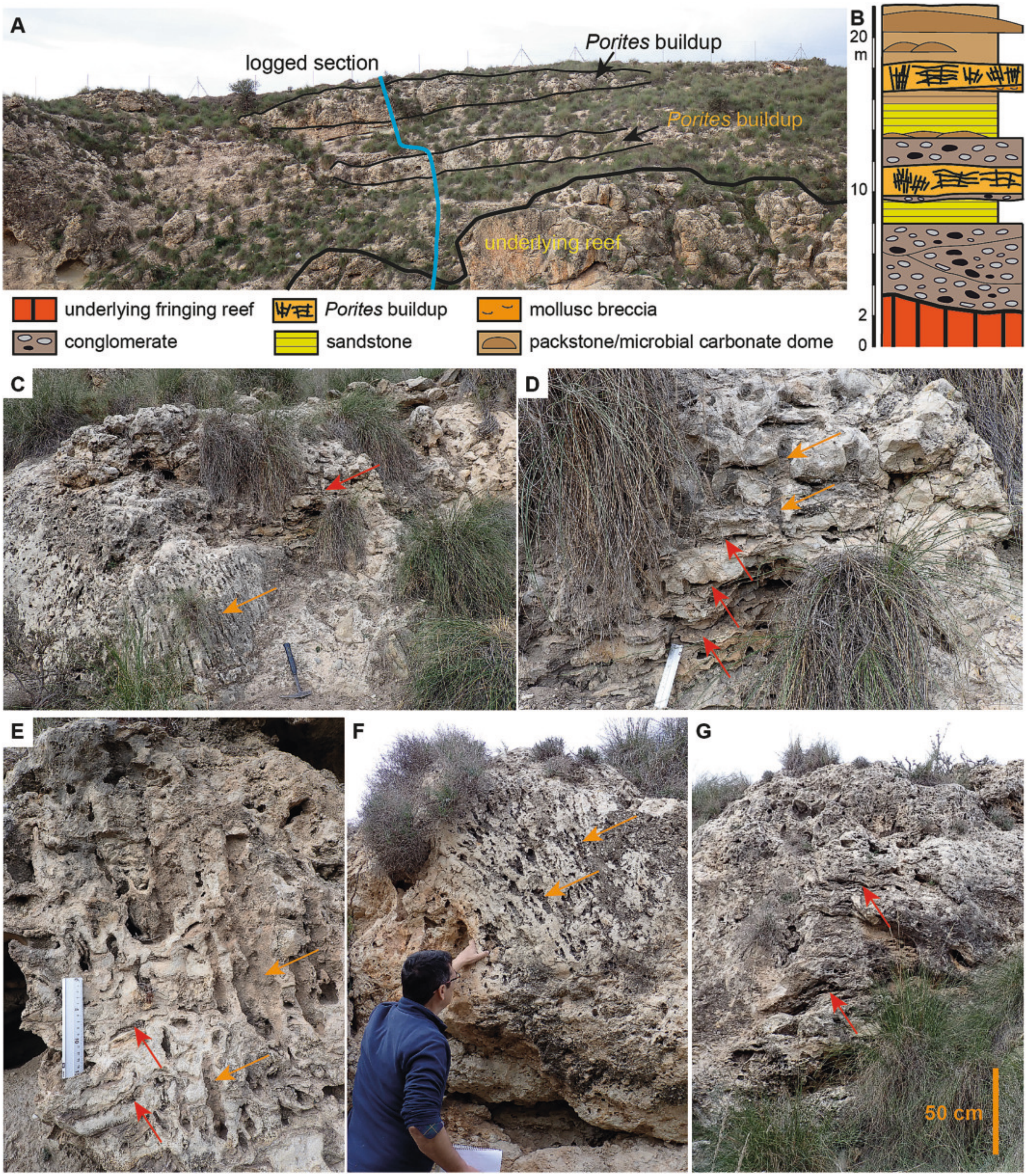

Fig. 8. View of the Rambla the Góchar outcrop of the TCC with coral buildups (see B for scale). B. Stratigraphic column (blue line in A). C. Colonies of columnar *Porites* (lower left quarter, orange arrow) overlain by laminar contorted *Porites* colonies with short finger-like projections (red arrow). Lower buildup. Hammer is 33 cm long. D. Close-up of laminar contorted *Porites* colonies (red arrows) with short finger-like projections (orange arrows) in A. Lower buildup. Ruler is 15 cm long. E. Colony of columnar *Porites* (orange arrows) with small laminar subhorizontal bridges (red arrows). Lower buildup. Ruler is 15 cm long. F. Branching-columnar *Porites* colony (orange arrows) in the upper buildup. Notebook is 21 cm long. G. Laminar contorted *Porites* colonies (red arrows) in the upper buildup. Note that *Porites* skeletons in pictures C to G are partially to totally dissolved and preserved at the surface as empty tubes and laminar voids. (For interpretation of the references to colour in this figure legend, the reader is referred to the web version of this article.)

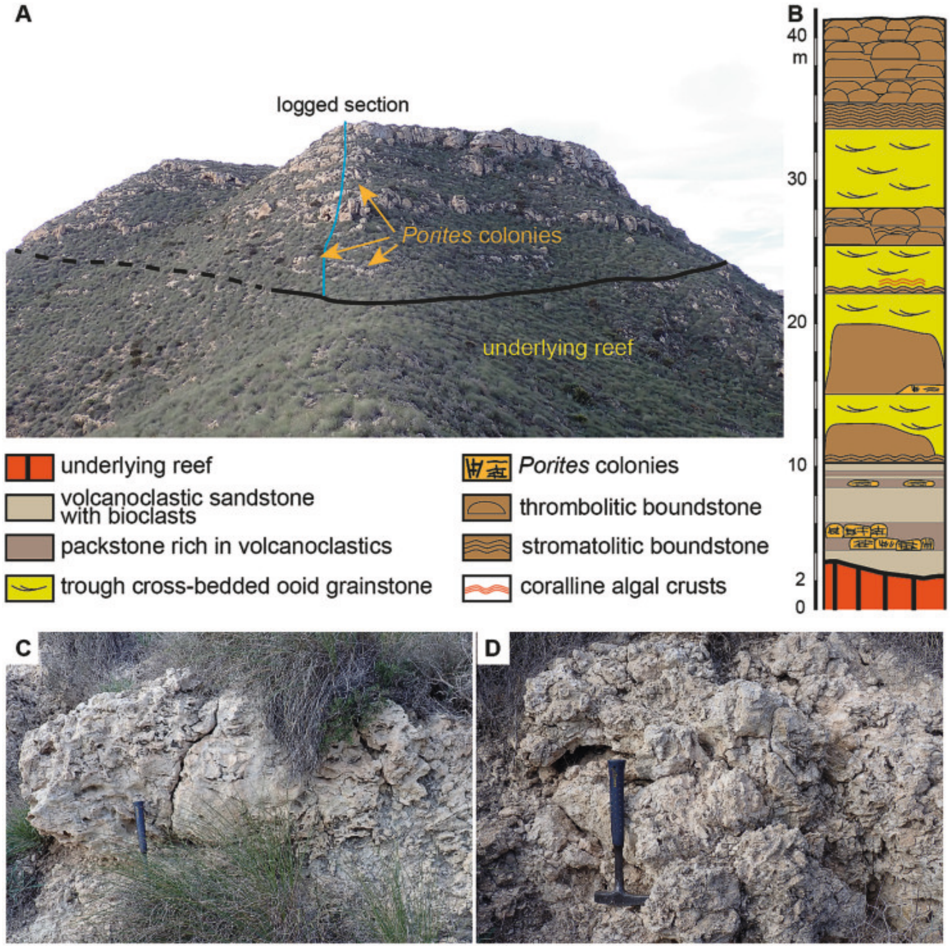

Fig. 9. A. View of the TCC outcrop at La Molata from the NE and location of the logged section in B (see column for scale). B. Stratigraphic column of the logged section. C. Laminar contorted *Porites* colonies (red arrows) partially dissolved and preserved as partially to totally empty voids in a volcanoclastic/bioclastic matrix. Hammer is 33 cm long. D. Columnar *Porites* colony in life position preserved as external moulds in a volcanoclastic/bioclastic matrix (orange arrows). Hammer is 33 cm long. (For interpretation of the references to colour in this figure legend, the reader is referred to the web version of this article.)

At the base of the logged column (Fig. 9B), laminar contorted *Porites* colonies (Fig. 9C), a few dm thick and wide occur together with fragments of columnar *Porites* colonies in a volcanoclastic/bioclastic matrix with small benthic foraminifera and coralline algal fragments. Individual laminae are less than 1 cm in thickness. Locally columnar *Porites* colonies, up to 50 cm high, are preserved in growth position (Fig. 9D). Individual columns are 2–3 cm in diameter. The corals are lined by coralline algae belonging to the order Hapalidiales and microbialite. The coral skeletons were partially to totally dissolved, and voids were partially filled by carbonate cement or remained empty. These deposits have a thickness of 2.70 m and are covered by 4.5 m of poorly exposed sandy silts with volcanoclastic and bioclastic grains intercalating cm-scale packstone beds and small laminar *Porites* colonies at about 3 m from their base. These soft sediments are capped by silty stromatolites, 0.2 m thick, followed by a lens-shaped thrombolitic boundstone, up to 2.3 m thick, extending laterally for about 12 m. The boundstone is rich in ooids and sand-sized bioclasts and changes laterally to trough cross-bedded ooid grainstones. Cross-bedded ooid grainstones, 8.5 m thick, engulf a bioherm of thrombolitic boundstone, up to 5 m thick, with a few columnar and laminar contorted *Porites* at the base. Among the overlying ooid grainstone, 4.5 m in thickness, a dome-like structure consists of stromatolitic boundstone, 50 cm thick, and coralline algal boundstone built by superimposition of thin encrusting to warty algal thalli of Hapalidiales. The succession continues with an alternation of ooid grainstone and microbial boundstone, about 16 m thick in the logged section. Goldstein et al. (2013) report the occurrence of a small *Porites* boundstone among ooid grainstone some 10 m below the succession top.

4.2.2. La Rellana

The TCC at La Rellana drapes and onlaps a palaeotopographic relief carved in the underlying lower Messinian reefs (Fig. 10A) (Goldstein et al., 2013). These authors distinguish four sequences within the TCC, the third of which includes many coral buildups among cross-bedded ooid grainstones. Although no specific datings have been performed for the TCC in this locality, Goldstein et al. (2013) and Lipinski et al. (2013) assumed that it is a lateral equivalent of the TCC in La Molata.

In the logged section (Fig. 10B) the erosion boundary surface is overlain by trough cross-bedded and planar-bedded ooid grainstone, 7.2 m thick, rich in volcanoclastics in the upper 1.5 m. These grainstones are followed by a thrombolitic boundstone, 2.3 m in thickness, forming amalgamated domes, 0.4–0.5 m thick and about 1 m wide. The succession continues with 3.9 m of trough cross-bedded ooid grainstone, intercalating a thin bed of stromatolites near the top. Stick *Porites* colonies settled directly on the ooid grainstones. Colonies are about 1 to 2 m high and a few decimetres to 2 m wide. Sticks are 1.5–2.5 cm in diameter and are bridged by short laminar growths less than 1 cm thick. The lower 4 m of the buildup consist of stacked upright coral colonies. Ooid grainstones covered the sides of the colonies and, in the upper 3.5 m of the buildup, interfingered with them (Fig. 10C). In this upper part, colonies up to 1 m high occur in growth position, tilted down or lying horizontally among the ooid grainstone (Fig. 10C). A stick *Porites* colony exposed some hundred metres south of the logged section is 2.6 m high

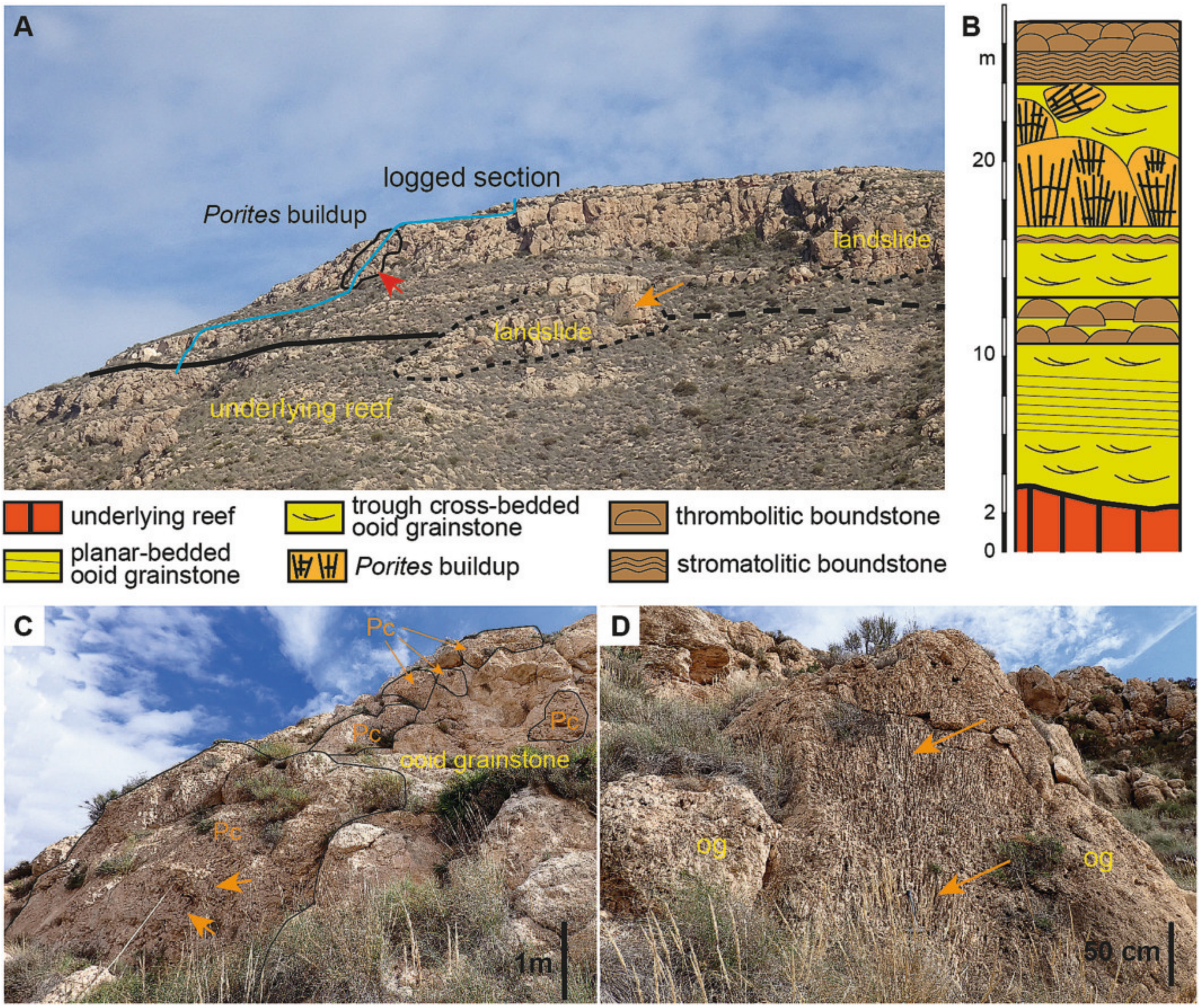

Fig. 10. A. View of the TCC outcrop at La Rellana from the W and location of the logged section in B (see column for scale). Red arrow points to buildup in C. Orange arrow points to *Porites* colony in D (see stratigraphic column for scale). B. Stratigraphic column of the logged section. C. *Porites* buildup formed by stacking of columnar colonies (Pc) some of them fallen down, interfingering with ooid grainstone. D. Stick *Porites* colony surrounded by ooid grainstone (og) in the small landslide south of the logged section. *Porites* skeletons in C and D are partially to totally dissolved and preserved as empty tubes (arrows). (For interpretation of the references to colour in this figure legend, the reader is referred to the web version of this article.)

and 1.8 m wide (Fig. 10D). Corals were encrusted by coralline algae and foraminifers, followed by microbialite with common stromatolitic fabrics. The coral skeletons are partially to totally dissolved. The internal sediment consists of bioclasts of molluscs, coralline algae and foraminifera, and ooids. The buildup is overlain by stromatolites, 1.6 m thick, followed by thrombolitic boundstone at the section top.

4.2.3. Mesa de Roldán

The TCC overlies an erosion surface carved on Messinian reefs (Fig. 11A) (Riding et al., 1991a). The surface is covered by a thin and discontinuous breccia of rounded and angular clasts from the underlying reef limestone, which is followed by a cross-bedded ooid grainstone, up to 2 m thick (Fig. 11B). The grainstone is overlain by a *Porites* buildup, up to 4 m thick, formed by stacked stick colonies with horizontal laminar growths bridging the sticks (Fig. 11C, D). Colonies are up to 2 m high (Fig. 11C) and individual sticks are 1–2 cm in diameter (Fig. 11D, E). The scarce sediment between colonies is a bioclastic packstone to rudstone rich in surficial ooids. The coral skeletons were encrusted by foraminifera, coralline algae, vermetids, serpulids, bryozoans and microbial crusts (Fig. 11E). Corals and encrusters show *Entobia* borings. *Lithophyllum* sp., *Titanoderma* gr. *pustulatum* (J.V.Lamouroux) Nägeli 1858, *Spongites* sp., and *Harveylithon* sp. can be identified as encrusting coralline algae. The matrix filling the framework voids (Fig. 11E) is a packstone to rudstone with fragments of bivalves, gastropods, echinoids, fish teeth, and small benthic foraminifers with coralline algal fragments and small fruticose nodules of *Lithophyllum* sp. and *Lithothamnion* sp. with bryozoans. Locally in the upper part, thin laminar contorted *Porites* colonies, less than 1 cm thick, coated by coralline algae and thick microbialite crusts (Fig. 11F) cap the stick colonies. The bioherm is overlain by a cross-bedded ooid grainstone, 4 m in thickness.

4.3. Post-evaporitic coral buildups in the Salento Peninsula

The Salento Peninsula-TCC (SP-TCC) consists of the superimposition of three main subunits. It crops out on both sides of the Leuca harbour (Fig. 6b), where it displays markedly different depositional facies

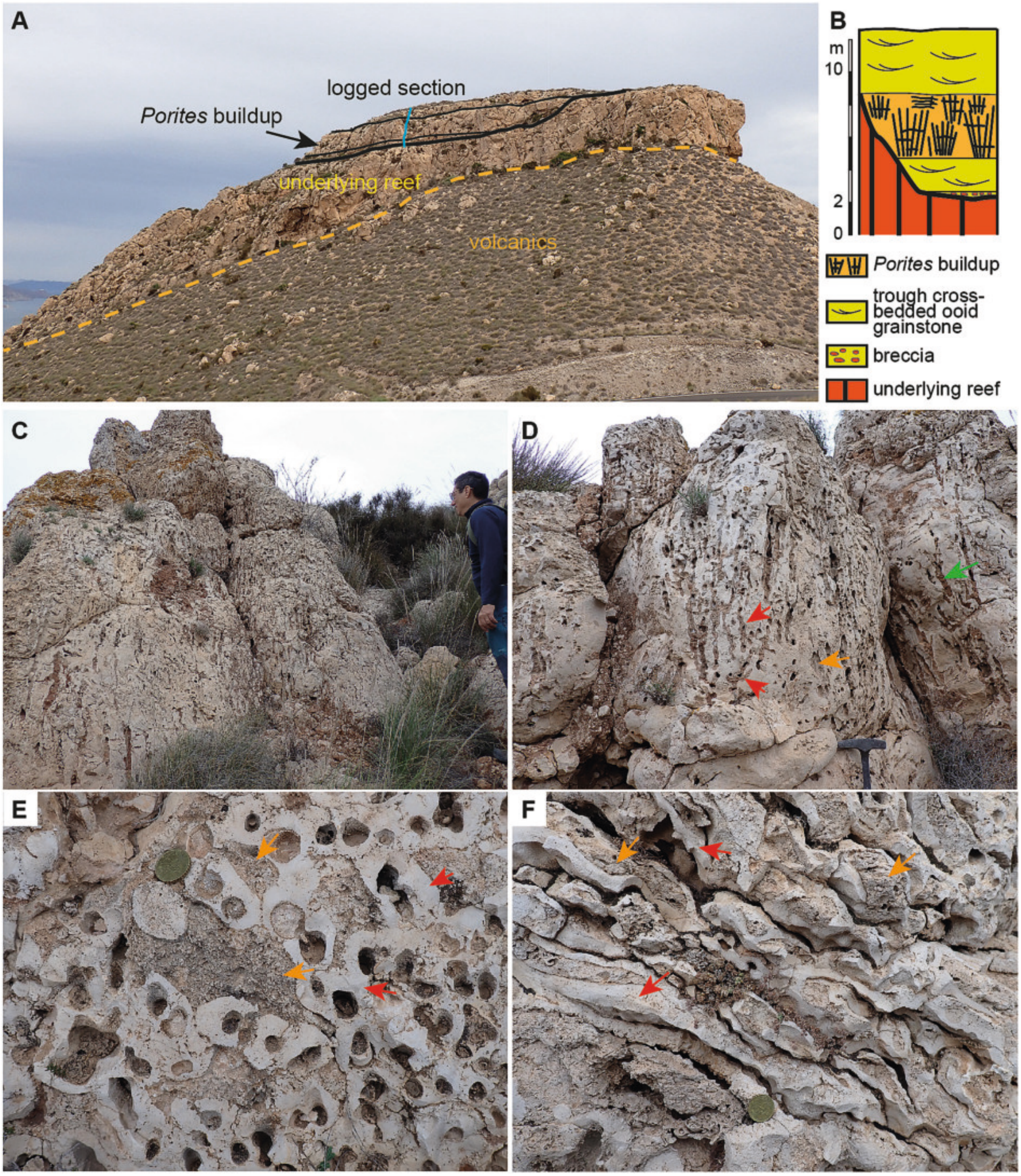

Fig. 11. A. View of the TCC outcrop at Mesa de Roldán from the S and location of the logged section in B (see column for scale). C. The buildup was made by stacked metre-scale stick *Porites* colonies. FS is 1,80 m tall. D. Stick *Porites* colonies. The coral skeletons were dissolved, and the voids remained empty (orange arrow) or were partially filled by late cements (red arrows) or karst deposits (green arrow). Hammer head is 18 cm long. E. Transverse section of stick *Porites* (empty voids) encrusted by microbial carbonate (red arrows). The spaces left by the framework builders were filled by packstone to rudstone with ooids (orange arrows). Coin diameter is 24 mm. F. Laminar contorted *Porites* (empty voids) encrusted by microbial carbonate (red arrows). The spaces left by the framework builders were filled by packstone to rudstone with ooids (orange arrows). Coin diameter is 24 mm. (For interpretation of the references to colour in this figure legend, the reader is referred to the web version of this article.)

(Vescogni et al., 2022).

At the western corner, north-west of Punta Ristola, sedimentation is predominantly oolitic/bioclastic and reaches about 12 m in thickness (Fig. 7). Each subunit starts with a very thin layer of marly limestone, followed by mollusc packstone–grainstone deposits that grade landward into ooid grainstone. Occasionally, these two facies contain very thin horizons of laminated peloidal stromatolite. The described coral buildup crops out within the ooid grainstone of the second subunit, subsequently capped by layers of fine-grained foraminiferal packstone (Fig. 7).

On the eastern side of the Leuca Gulf, just north of Leuca Cape, the SP-TCC exhibits approximately 6 m of thickness and is characterised by a more proximal/protected depositional environment. In this case, sedimentation is dominated by microbialites, displaying several different facies, some of which have not previously been recorded in the late Messinian of the Mediterranean (Vescogni et al., 2022, 2025). Microbial boundstones are here associated mainly to marly mudstone/wackestone and ooid grainstone. At the Leuca Cape a clear identification of the three SP-TCC subunits is hampered by the reduced thickness of the succession and by the marked erosive nature of the boundaries separating most of the depositional facies.

In the SP-TCC, *Porites* fragments can be found scattered within the ooid grainstone on both sides of Leuca Harbour, but the only discrete coral buildup has been identified at Punta Ristola (Figs. 6b, 7). This structure crops out over a length of 52 m and reaches a thickness of approximately 4.8 m (Fig. 12a, b). It overlies massive breccia deposits (Fig. 12i)., up to some decimetres thick, composed of angular to more rounded clasts derived from the underlying massive to slightly stratified ooid grainstones, which display horizontal-parallel and cross lamination. The ooid grainstone also laterally surrounds and partially overlies the coral buildup, which on its NNW side is covered by fine-grained foraminiferal packstone. A wide channel, filled by stratified bioclastic packstone-rudstone, cuts through the coral buildup, dividing it into two distinct sections.

The buildup has a massive structure and is characterised by the presence of colonies of *Porites* and *Siderastrea* in growth position. *Porites* is the most abundant coral genus, represented by branching to columnar colonies. They reach several decimetres in size, with an average branch diameter of approximately 2.5 cm, occasionally up to 6 cm (Fig. 12c-e). Individual branches often fuse laterally (Fig. 12c) and significantly strengthen the overall structure of the colony. *Siderastrea* is instead represented by smaller spherical to ellipsoidal growth-forms, with an average size of a few centimetres (Fig. 12f). Diagenesis and surface alteration have led to a profound alteration of the coral microstructures, and colonies of both genera are usually preserved as moulds. Nonetheless, some specimens with relatively good preservation still retain evidence of fine calicular structures (Fig. 12e, f). In some cases, both *Porites* and *Siderastrea* colonies are lined by thin crusts of coralline red algae (Fig. 12f) and encrusting foraminifera. Coral colonies do not form a continuous skeletal framework, instead they occur in small clusters or are scattered throughout the buildup. Inter-colony sediment consists of prevalent grainstone-packstone (Fig. 12g, h) with horizontal-parallel to cross lamination (Fig. 12l) and traces of bioturbation, composed mainly of small pellets, often coated by thin oolitic rims, as well as coral remains and small fragments of the underlying ooid grainstone. Less abundant skeletal grains include gastropods, small benthic foraminifera (primarily miliolids, but also *Ammonia* and *Elphidium*), brachiopods, bivalves, serpulids, coralline algae, echinoderms, and rare dasycladaleans. In proximity to the branching *Porites* colonies, sediment pockets with mud-supported textures may also occur; these are usually bioturbated mudstone–wackestone containing pellets, coral fragments, and mollusc

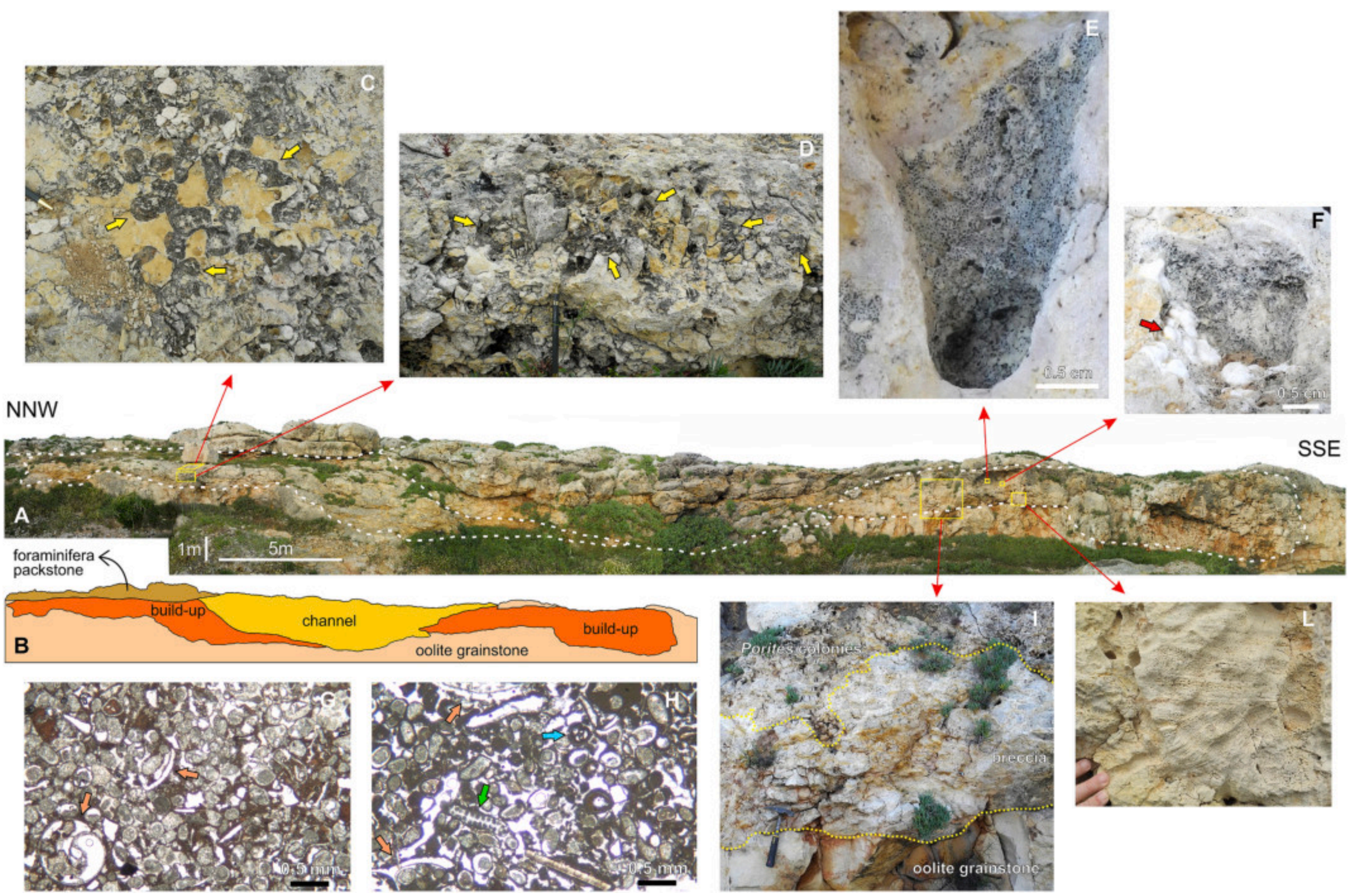

Fig. 12. Salento Peninsula buildup. A. Outcrop view of the *Porites* buildup; white dashed lines indicate the upper and lower boundaries of the buildup, as well as its contact with the channel that cuts across it. B. Schematic representation of A highlighting geometry of the *Porites* buildup and the associated lithologies. C, D. Outcrop close-ups of a branching *Porites* colony, cut perpendicularly and parallel to the growth direction, respectively. Coral branches (yellow arrows) are preserved as moulds and appear darker than the surrounding sediment. E. Outcrop close-ups of a *Porites* branch partially preserving its microstructure. F. Outcrop close-ups of a *Siderastrea* colony partially preserving its microstructure; red arrow indicates a thin coating of coralline red algae. G, H. Thin sections of the grainstone-packstone among the coral colonies, with prevalent pellets associated to gastropod remains (orange arrows), miliolids (blue arrow) and dasycladalean fragments (green arrow). I. Outcrop view of the lower boundary of the *Porites* buildup, showing the basal ooid grainstone and the breccia deposits that mark the transition to coral colonisation. L. Outcrop close-up of cross lamination within the sediment among coral colonies. (For interpretation of the references to colour in this figure legend, the reader is referred to the web version of this article.)

remains.

5. Discussion

5.1. Palaeoenvironments of upper Messinian coral buildups

The Messinian post-evaporitic corals grew in diverse settings. In the TCC in the Sorbas Basin they developed among mainly siliciclastic deposits in a small fan delta at the shelf break defined by the topography of the underlying erosion surface that follows the geometry of the lower Messinian fringing reefs. A certain degree of turbidity caused by sediment load probably conditioned the coral growth forms, dominated by relatively small columnar and laminar contorted *Porites* colonies. Small, laminar contorted colonies with a few finger-like projections and rare small stick colonies of *Porites* among sandy silts and volcanoclastic/bioclastic sediment also reflect a turbid environment during coral growth in the first steps of the marine flooding of the erosion surface carved in the lower Messinian reefs in La Molata. The branching growth form is largely considered the most effective with respect to sediment clearance by passive removal in turbid environments (Stafford-Smith, 1993; Novak et al., 2013; Santodomingo et al., 2015; Bosellini et al., 2024); whereas the laminar-platy morphology is well adapted to a reduced light penetration that can be caused by high turbidity (Rosen et al., 2002; Reuter et al., 2019). The occurrence of only Hapalidiales in the CCA crusts around coral skeletons and in the CCA crusts growing on microbialite boundstone also indicates a poorly illuminated setting.

In contrast, in Mesa de Roldán and La Rellana the exuberant growth of stick *Porites* colonies more than 1 m tall took place in clear waters among oolite shoals in the shelves at the top of the underlying lower Messinian reefs, which developed on volcanic highs. The La Rellana logged example shows that the lateral and vertical extension of coral buildups was limited by the ooid grainstone that surrounded them, totally or partially burying the bioherms and engulfing isolated coral colonies. Goldstein et al. (2013) interpreted the trough cross-bedded ooid grainstones surrounding the buildups as shallow-water (< 10 m deep) deposits accumulated in high-energy conditions above fair-weather wave base in the shoreface of a beach system represented by the underlying tabular and trough cross-bedded ooid grainstones. The depositional setting opened eastward to the Mediterranean Sea.

In Rambla de Góchar, La Molata, and La Rellana, corals occur intercalated with microbial boundstones. According to Goldstein et al. (2013), in La Molata and La Rellana, thrombolitic boundstones formed in high-energy, normal-marine shallow waters, based on their association with cross-bedded ooid grainstones and a diverse faunal assemblage. The same authors suggest that stromatolitic boundstones probably developed under more restricted marine conditions. Bourillot et al. (2020) proposed low-energy, normal-marine to hypersaline conditions for the formation of stromatolitic boundstones, and high-energy, normal-marine to hypersaline settings for the dominantly thrombolytic microbialites in the Sorbas TCC. Microbial boundstone domes, including stromatolites, are forming today in oolitic shoals in normal-marine waters in Bahamian cays (Dill et al., 1986; Riding et al., 1991c; Andres et al., 2006). By analogy with this modern example, normal-marine conditions were interpreted for microbial boundstone domes in the TCC of the Sorbas Basin (Martín et al., 1993; Braga et al., 1995), and for stromatolitic and thrombolitic boundstone domes in the TCC of Níjar, a locality in the Níjar–Almería Basin near the Cabo de Gata area (Riding et al., 1991a). The coral buildups in Salento also grew in a narrow shelf on top of an erosion surface cutting lower Messinian reefs and older carbonate rocks. Similarly to the Mesa de Roldán and La Rellana examples, the Salento *Porites* colonies are relatively large and grew surrounded by horizontal-parallel to cross-bedded ooid packstone-grainstone. These features thus suggest a comparable depositional setting, characterised by high-energy, shallow-water conditions. The occurrence in both cases of echinoids and a diverse mollusc assemblage, and dasycladalean algae in the Salento outcrop, indicates salinity values comparable to normal marine conditions.

5.2. Implications for models of MSC events: timing and palaeoenvironments

The stratigraphic relationships in the Sorbas Basin demonstrate that the coral buildups in the TCC postdate the Messinian evaporites in the basin and are late Messinian in age. However, a crucial question to address is the temporal relationship of the TCC in Sorbas and the TCC in Cabo de Gata and Salento with the salt in the deep Mediterranean Basin. The lack of enough resolution of correlations leaves open to interpretation the exact relative position of carbonates, evaporites and erosion surfaces in the emergent basins and evaporite formation in the deep basins. Different models of the Mediterranean evolution during the Messinian propose substantially different temporal schemes.

According to Riding et al. (1998, 1999), Braga et al. (2006) and Bourillot et al., 2020, the Sorbas Basin record reflects a major drawdown of sea level after deposition of lower Messinian coral reefs at the basin margins and pelagic marls in the basin centre. This sea-level fall caused the subaerial erosion surface below the Yesares gypsum in the centre (Riding et al., 1998, 1999; Braga et al., 2006), which continues below the TCC at the margins with an observable relief up to 240 m between the top of the fringing reefs and the base of the gypsum. The relief of the erosion surface indicates a significant minimum drawdown with respect to the Atlantic Ocean and was the time equivalent of deep desiccation of the adjacent Mediterranean Basin (Riding et al., 1998, 1999; Braga et al., 2006). Bourillot et al. (2010a, 2020) also correlate this surface with the major MSC drawdown and precipitation of the lower evaporite in the Mediterranean Basin. This interpretation is followed by Goldstein et al. (2013) and Lipinski et al. (2013) for the subaerial erosion surface underlying the TCC in Cabo de Gata, which exhibits a palaeotopographic relief of 76 m in La Rellana. The Yesares Gypsum formed during the reflooding of the basin by marine waters. Gypsum beds alternate with fine-grained siliciclastics that contain normal-marine fossil assemblages in the last alternations (Saint-Martin et al., 2000). The marine reflooding continued after the last evaporite precipitation and the post-evaporite deposits onlapped the slopes of lower Messinian reefs at the basin margins until the flooding of shelves on top of the pre-evaporitic reefs. On these shelves and on those in Cabo de Gata and Salento grew the post-evaporitic corals forming buildups among fan-delta sediments or among oolite shoals. According to this series of events, the corals in the TCC postdate the main episode of desiccation of the Mediterranean Basin. Although *Porites* is one of the zooxanthellate corals with higher levels of halotolerance and lives in wide ranges of temperature and turbidity (Halfar et al., 2005; Padilla-Gamiño et al., 2012; Huang et al., 2025; Samperiz et al., 2025), it is obvious that the occurrence of zooxanthellate coral buildups and associate faunas and floras in SE Spain and Salento implies the existence of marine waters all over the central and western Mediterranean basin during an interval in the late Messinian. Sea-level reached higher or similar elevations to those during development of the pre-evaporitic reefs as the TCC deposits lie on top of the shallowest facies of the underlying bioconstructions. This means that the growth of the TTC corals took place during the highest relative sea level in the Mediterranean Messinian, making difficult assuming any kind of coeval evaporite precipitation both in the Sorbas Basin (Conesa et al., 1999; Cornée et al., 2004; Roveri et al., 2009) or in the deep Mediterranean Basin. The Gibraltar Straits seem to have been the gate to fill the Mediterranean Basin with oceanic waters from the Atlantic (Krijgsman et al., 2018; Roveri et al., 2025).

After this late Messinian marine episode, the Sorbas Basin emerged and was occupied by a fluvial system with small ephemeral lakes (Mather, 1991; Mather and Stokes, 2001). A last marine invasion of the basin took place in the earliest Zanclean (Roveri et al., 2019) before a final emersion with development of continental deposits until the end of the basin fill in the Early Pleistocene (Stokes et al., 2018). A rather similar evolution appears to have characterised the upper Messinian succession in Salento as well. There, the TCC is followed by an erosional phase and by the emplacement of the upper Messinian Leuca Breccia Formation. The final marine ingression is subsequently documented by marly deposits dated to the middle Zanclean (Bosellini et al., 1999).

The timing of events of Mediterranean evolution during MSC proposed by Krijgsman et al. (1999), Rouchy and Caruso (2006), CIESM (Comm. Int. Explor. Sci. Méditerr.) (2008), Roveri et al. (2014, 2025) are not consistent with the occurrence of post-evaporitic zooxanthellate coral buildups as they ignore such occurrence and the presence of marine waters all over the western and central Mediterranean during at least an interval in the late Messinian. All those authors state that all deposits formed in the region after the Sorbas evaporites, considered either as Lower Evaporites (i.e. Krijgsman et al., 1999; Rouchy and Caruso, 2006) or as Primary Lower Gypsum (i.e. CIESM (Comm. Int. Explor. Sci. Méditerr.), 2008; Roveri et al., 2014, 2025), were evaporites or brackish sediments (Lago Mare) until the return of marine conditions in the Zanclean. In a similar way, stratigraphies of the Sorbas Basin, and their correlation with other Mediterranean basins, which locate an erosion surface equivalent to the major drawdown event of the MSC between the TCC/Sorbas Member and the overlying Zorreras (Krijgsman et al., 2001; Meilijson et al., 2019) are also not consistent with our observations. They overlook the marine nature of at least part of the TCC/Sorbas Member and the lack of any erosion surface separating both members (Martín and Braga, 1994; Martín et al., 1993; Riding et al., 1998; Bourillot et al., 2010b, 2020). Clauzon et al. (2015) also omit the occurrence of post-evaporitic corals. These authors propose an erosion surface between the Yesares Gypsum and the TCC/Sorbas Member that is not supported by field observations in well-exposed basin sections. Similarly, the model proposed by Garcia-Castellanos et al. (2025) is inconsistent with the Sorbas Basin record as they postulate a kilometric drawdown of Mediterranean Sea level postdating the Yesares Gypsum, which is not reflected by any erosion surface in the sedimentary succession in the basin. This model does not account for the occurrence of coral reefs and marine waters in the Mediterranean Basin in the late Messinian.

5.3. The recovery of zooxanthellate corals

The question of how zooxanthellate corals, and *Porites* in particular, reappeared in the Mediterranean after evaporite deposition associated with the MSC was first addressed by Esteban (1979), who proposed two alternatives: either *Porites* survived the crisis within the basin, or it re-entered the Mediterranean after marine conditions returned. Esteban (1979) considered both hypotheses problematic, noting that the persistence of *Porites* under hypersaline conditions seemed unlikely and that no clear external source for recolonisation could be identified.

Subsequent research has provided a more nuanced framework for evaluating these possibilities. Analyses of the geographic distribution of zooxanthellate coral genera during the Late Miocene revealed that certain areas, particularly those bordering the Betic–Balearic region and North Africa, stood out for their consistently high coral generic richness from the Tortonian into the early Messinian (Perrin and Bosellini, 2013). According to these authors, one possible explanation of the reappearance of *Porites* could be related to the persistence of open-marine conditions either for longer periods or continuously within small basins in the western Mediterranean. Those semi-isolated marine basins could have acted as refugia for marine biotas during the most hypersaline stages of the crisis, offering suitable habitats for the survival of *Porites*. *Porites* possess intrinsic biological properties and a remarkable capacity for ecological flexibility and stress tolerance, traits that continue to characterise the genus today, as demonstrated by the occurrence of high-latitude monospecific *Porites* communities (Halfar et al., 2005). We postulate that the occurrence of upper Messinian *Porites* buildups in the Salento Peninsula in the central Mediterranean suggests that zooxanthellate corals did not completely disappear and later recolonised the area over long distances but instead survived in localised refugia. In this sense, the hypothesis of Booth-Rea et al. (2018) of the occurrence of a main sill between the Atlantic and the Mediterranean located in the volcanic arc of the East Alboran Basin and the persistence of marine waters in the West Alboran Basin throughout the MSC would have provided a perfect scenario for the maintenance of *Porites* in the Mediterranean region and its rapid recolonisation of shallow-shelf habitats in the late Messinian after drawdown episodes. This hypothesis was questioned based on geophysical evidence and palaeotopographic reconstructions of the Alboran Basin by Heida et al. (2024). However, the results of scientific drilling in the West Alboran Basin (site U1611, IODP Expedition 401) support the persistence of marine conditions in the area from 6.4 Ma (early Messinian) to the base of the Zanclean (Flecker et al., 2025), i.e., before, during, and after the MSC. The recovered deposits from this interval mainly consist of continuous succession of mud to silty sands, with nannoplankton and planktonic foraminifers present in most samples (Flecker et al., 2025). At present, until the Messinian evolution of the Western Alborán Basin is better defined and this basin (or basins) can be properly identified as a potential refugium during the MSC, the within-basin survival hypothesis remains speculative, and recolonization of the Mediterranean Basin from the eastern Atlantic cannot be completely ruled out.

6. Conclusions

Late Messinian post-evaporitic zooxanthellate coral buildups occur in the Terminal Carbonate Complex in the Sorbas Basin and in the Cabo de Gata are in SE Spain and in the Salento Peninsula in SE Italy. These buildups are structures metres to tens of metres wide and decimetres to a few metres high, which grew among fan-delta mixed siliciclastic-carbonate sediments and in oolite shoals in shallow high-energy shelf settings developed on top of an erosion surface carving lower Messinian reefs. *Porites* is the only recorded builder in SE Spain, while minor *Siderastrea* colonies occur in Salento. Echinoids, diverse molluscs and coralline and dasycladalean algae appear in the sediments surrounding or infilling the coral frameworks. The post-evaporitic coral buildups imply the existence of normal marine waters all over the western and central Mediterranean during at least one interval in the late Messinian after evaporite deposition. Sea level reached the elevation of lower Messinian reefs during this post-evaporitic marine episode, refuting hypothesis of coeval evaporite formation in the Sorbas Basin or in the deep Mediterranean Basin. Consequently, the occurrence of zooxanthellate corals challenges models of Mediterranean evolution that do not account for complete marine reflooding of the central and western Mediterranean in the late Messinian. The source of zooxanthellate corals for recolonisation after evaporite deposition remains elusive. Their occurrence in Salento favours the hypothesis of survival in within-basin refugia in the western Mediterranean region but a dispersion from the Atlantic cannot be totally excluded.

CRediT authorship contribution statement

Juan C. Braga: Writing – original draft, Investigation, Conceptualization. **Alessandro Vescogni:** Writing – review & editing, Investigation, Conceptualization. **Fernando Sola:** Writing – review & editing, Investigation, Conceptualization. **Francesca R. Bosellini:** Writing – review & editing, Investigation, Conceptualization. **Julio Aguirre:** Writing – review & editing, Investigation, Conceptualization.

Declaration of competing interest

The authors declare that they have no known competing financial interests or personal relationships that could have appeared to influence the work reported in this paper.

Acknowledgements

We are grateful to J.-J. Cornée, an anonymous reviewer, guest editor Daniela Basso and editor Lucia Angiolini for their detailed and valuable comments, which helped to improve the first version of this paper. The work of JCB and JA was partially funded by the "Ministerio de Ciencia, Innovación y Universidades" of Spain, project PID2022.142806NB.100, and the Junta de Andalucía Research Group RNM 190.

Data availability

The authors confirm that all data necessary for supporting the scientific findings of this paper have been provided.

References

Agiadi, K., Hohmann, N., Gliozzi, E., Thivaiou, D., Bosellini, F.R., Taviani, M., Bianucci, G., Collareta, A., Londeix, L., Faranda, C., Bulian, F., Koskeridou, E., Lozar, F., Mancini, A.M., Dominici, S., Moissette, P., Bajo-Campos, I., Borghi, E., Iliopoulos, G., Antonarakou, A., Kontakiotis, G., Besiou, E., Zarkogiannis, S., Harzhauser, M., Sierro, F.J., Coll, M., Vasiliev, I., Camerlenghi, A., Garcia-Castellanos, D., 2024a. Late Miocene transformation of Mediterranean Sea biodiversity. Sci. Adv. 10, eadp1134.

Agiadi, K., Hohmann, N., Gliozzi, E., Thivaiou, D., Bosellini, F.R., Taviani, M., Bianucci, G., Collareta, A., Londeix, L., Faranda, C., Bulian, F., Koskeridou, E., Lozar, F., Mancini, A.M., Dominici, S., Moissette, P., Bajo-Campos, I., Borghi, E., Iliopoulos, G., Antonarakou, A., Kontakiotis, G., Besiou, E., Zarkogiannis, S., Harzhauser, M., Sierro, F.J., Coll, M., Vasiliev, I., Camerlenghi, A., Garcia-Castellanos, D., 2024b. The marine biodiversity impact of the Late Miocene Mediterranean salinity crisis. Science 385, 986–991.

André, J.P., Cornée, J.J., Saint Martin, J.P., Lapointe, P., 2002. Organisation séquentielle de la plate-forme carbonatée messinienne du seuil pélagien à Lampedusa (Méditerranée centrale). Geodiversitas 24 (3), 625–639.

Andres, M.S., Sumner, D.Y., Reid, R.P., Swart, K.P., 2006. Isotopic fingerprints of microbial respiration in aragonite from Bahamian stromatolites. Geology 34 (11), 973–976. https://doi.org/10.1130/G22859A.1.

Betzler, C., Martín, J.M., Braga, J.C., 2000. Non-tropical carbonates related to rocky submarine cliffs (Miocene, Almería, southern Spain). Sediment. Geol. 131 (1–2), 51–65.

Booth-Rea, G., Ranero, C.R., Grevemeyer, I., 2018. The Alboran volcanic-arc modulated the Messinian faunal exchange and salinity crisis. Sci. Rep. 8, 13015.

Bosellini, F.R., 2006. Biotic changes and their control on Oligocene–Miocene reefs: a case study from the Apulia Platform margin (southern Italy). Palaeogeogr. Palaeoclimatol. Palaeoecol. 241, 393–409.

Bosellini, A., Parente, M., 1994. The Apulia Platform margin in the Salento Peninsula (southern Italy). Giorn. Geol. 56, 167–177.

Bosellini, F.R., Perrin, C., 2008. Estimating Mediterranean Oligocene–Miocene sea-surface temperatures: an approach based on coral taxonomic richness. Palaeogeogr. Palaeoclimatol. Palaeoecol. 258, 71–88.

Bosellini, A., Bosellini, F.R., Colalongo, M.L., Parente, M., Russo, A., Vescogni, A., 1999. Stratigraphic architecture of the Salento coast from Capo d'Otranto to S. Maria di Leuca (Apulia, southern Italy). Riv. Ital. Paleont. S. 105, 397–416.

Bosellini, F.R., Russo, A., Vescogni, A., 2001. Messinian reef-building assemblages of the Salento Peninsula (southern Italy): palaeobathymetric and palaeoclimatic significance. Palaeogeogr. Palaeoclimatol. Palaeoecol. 175, 7–26.

Bosellini, F.R., Russo, A., Vescogni, A., 2002. The Messinian reef complex of the Salento Peninsula (Southern Italy): stratigraphy, facies and paleoenvironmental interpretation. Facies 47, 91–112.

Bosellini, F.R., Vescogni, A., Budd, A., Papazzoni, C.A., 2021. High coral diversity is coupled with reef-building capacity during the late Oligocene warming (Castro Limestone, Salento Peninsula, S Italy). Riv. Ital. Paleont. S. 127 (3), 515–538.

Bosellini, F.R., Vescogni, A., Briguglio, A., Piazza, M., Papazzoni, C.A., Silvestri, G., Morsilli, M., 2024. Growth and demise of mesophotic coral buildups in a fan-delta system during the Late Oligocene Warming Event (Tertiary Piedmont Basin, NW Italy). In: Bottini, C., Crippa, G. (Eds.), Biocalcifier Resilience and Response during Global Climate Changes, 649. Palaeogeogr. Palaeoclimatol. Palaeoecol., p. 112330

Bossio, A., Mazzei, R., Monteforti, B., Salvatorini, G., 2002. Note illustrative alla carta geologica della zona di S. Maria di Leuca. Atti Società Toscana Scienze Naturali Mem. 107, 97–163.

Bourillot, R., Vennin, E., Kolodka, C., Rouchy, J.M., Caruso, A., Durlet, C., Chaix, Ch., Rommevaux, V., 2009. The role of topography and erosion in the development and architecture of shallow-water coral bioherms (Tortonian–Messinian, Cabo de Gata, SE Spain). Palaeogeogr. Palaeoclimatol. Palaeoecol. 281 (1–2), 92–114.

Bourillot, R., Vennin, E., Rouchy, J.M., Blanc-Valleron, M.M., Caruso, A., Durlet, C., 2010a. The end of the Messinian Salinity Crisis in the western Mediterranean: insights from the carbonate platforms of South-Eastern Spain. Sediment. Geol. 229 (4), 224–253.

Bourillot, R., Vennin, E., Rouchy, J.M., Durlet, C., Rommevaux, V., Kolodka, C., Knap, F., 2010b. Structure and evolution of a Messinian mixed carbonate-siliciclastic platform: the role of evaporites (Sorbas Basin, South-east Spain). Sedimentology 57, 477–512.

Bourillot, R., Vennin, E., Dupraz, C., Pace, A., Foubert, A., Rouchy, J.M., Patrier, P., Blanc, P., Bernard, D., Lesseur, J., Visscher, P.T., 2020. The record of environmental and microbial signatures in ancient microbialites: the terminal carbonate complex from the Neogene basins of southeastern Spain. Minerals 10 (3), 276.

Brachert, T.C., Hultzsch, N., Knoerich, A.C., Krautworst, U.M.R., Stückrad, O.M., 2001. Climatic signatures in shallow-water carbonates: high-resolution stratigraphic markers in structurally controlled carbonate buildups (Late Miocene, southern Spain). Palaeogeogr. Palaeoclimatol. Palaeoecol. 175 (1–4), 211–237.

Brachert, T.C., Krautworst, U.M.R., Stückrad, M., 2002. Tectono-climatic evolution of a Neogene intramontane basin (Late Miocene Carboneras subbasin, Southeast Spain): revelations from basin mapping and biofacies analysis. Basin Res. 14, 503–521.

Brachert, T.C., Vescogni, A., Bosellini, F.R., Reuter, M., Mertz-Kraus, R., 2007. High salinity variability during the early Messinian revealed by stable isotope signatures from vermetid and *Halimeda* reefs of the Mediterranean region. Geol. Romana 40, 51–66.

Braga, J.C., Martín, J.M., 1996. Geometries of reef advance in response to relative sea-level changes in a Messinian (uppermost Miocene) fringing reef (Cariatiz reef, Sorbas Basin, SE Spain). Sediment. Geol. 107 (1–2), 61–81.

Braga, J.C., Martin, J.M., Riding, R., 1995. Controls on microbial dome fabric along a carbonate-siliciclastic shelfbasin transect, Miocene, SE Spain. Palaios 10, 347–361.

Braga, J.C., Martín, J.M., Riding, R., 1996. Internal structure of segment reefs: Halimeda algal mounds in the Mediterranean Miocene. Geology 24 (1), 35–38.

Braga, J.C., Martín, J.M., Riding, R., Aguirre, J., Sánchez-Almazo, I.M., Dinarès-Turell, J., 2006. Testing models for the Messinian salinity crisis: the Messinian record in Almería, SE Spain. Sediment. Geol. 188, 131–154.

Braga, J.C., Vescogni, A., Bosellini, F.R., Aguirre, J., 2009. Coralline algae (Corallinales, Rhodophyta) in western and Central Mediterranean Messinian reefs. Palaeogeogr. Palaeoclimatol. Palaeoecol. 275, 113–128.

Calvet, F., Zamarreño, I., Vallès, D., 1996. Late Miocene reefs of the Alicante–Elche basin, Southeast Spain. In: Franseen, E.K., Esteban, M., Ward, W.C., Rouchy, J.M. (Eds.), Models for Carbonate Stratigraphy from Miocene Reef Complexes of Mediterranean Regions Soc. Econ. Paleontol. Mineral., Concepts Sedimentol. Paleontol. Ser, 5, pp. 177–190.

CIESM (Comm. Int. Explor. Sci. Méditerr.), 2008. The Messinian Salinity Crisis from Mega-deposits to Microbiology — A Consensus Report. Worksh. Monogr, 33. CIESM, Monaco.

Clauzon, G., Suc, J.P., Do Couto, D., Jouannic, G., Melinte-Dobrinescu, M.C., Jolivet, L., Quillévéré, F., Lebret, N., Mocochain, L., Popescu, S.-M., Martinell, J., Domenech, R., Rubino, J.-R., Gumiaux, C., Warny, S., Bellas, S.M., Gorini, C., Bache, F., Rabineau, M., Estrada, F., 2015. New insights on the Sorbas Basin (SE Spain): the onshore reference of the Messinian salinity crisis. Mar. Pet. Geol. 66, 71–100.

Conesa, G., Saint Martin, J.P., Cornée, J.J., Muller, J., 1999. Nouvelles contraintes sur la crise de salinité messinienne par l'étude d'une plate-forme carbonatée marginale (bassin de Sorbas, Espagne). CR Acad. Sci. Paris 328, 81–87.

Cornée, J.J., Saint Martin, J.P., Conesa, G., Münch, P., André, J.P., Saint Martin, S., Roger, S., 2004. Correlations and sequence stratigraphic model for Messinian carbonate platforms of the western and Central Mediterranean. Int. J. Earth Sci. 93 (4), 621–633.

Cornée, J.J., Ferrandini, M., Saint Martin, J.P., Münch, P., Moullade, M., Ribaud-Laurenti, A., Roger, S., Saint Martin, S., Ferrandini, J., 2006. The late Messinian erosional surface and the subsequent reflooding in the Mediterranean: new insights from the Melilla–Nador basin (Morocco). Palaeogeogr. Palaeoclimatol. Palaeoecol. 230 (1–2), 129–154.

Cornée, J.J., Maillard, A., Conesa, G., Garcia, F., Saint Martin, J.P., Sage, F., Münch, P., 2008. Onshore to offshore reconstruction of the Messinian erosion surface in Western Sardinia, Italy: implications for the Messinian salinity crisis. Sediment. Geol. 210 (1–2), 48–60.

Cuevas-Castell, J.M., Betzler, C., Roessler, J., Huessner, H., Peinl, M., 2007. Integrating outcrop data and forward computer modelling to unravel the development of a Messinian carbonate platform in SE Spain (Sorbas Basin). Sedimentology 54 (2), 423–441.

Cunningham, K.J., Benson, R.H., Rakic-El Bied, K., McKenna, L.W., 1997. Eustatic implications of late Miocene depositional sequences in the Melilla Basin, northeastern Morocco. Sediment. Geol. 107 (3–4), 147–165.

Dill, R.F., Shinn, E.A., Jones, A.T., Kelly, K., Steinen, R.P., 1986. Giant subtidal stromatolites forming in normal salinity waters. Nature 324, 55–58.

Dunham, R.J., 1962. Classification of carbonate rocks according to depositional texture. In: Hamm, W.E. (Ed.), Classification of Carbonate Rocks, a Symposium, 1. AAPG Mem., pp. 108–121

Embry, A.F., Klovan, J.E., 1971. A late Devonian reef tract on northeastern Banks Island, NWT. Bull. Can. Petrol. Geol. 19 (4), 730–781.

Esteban, M., 1979. Significance of the Upper Miocene coral reefs of the western Mediterranean. Palaeogeogr. Palaeoclimatol. Palaeoecol. 29, 169–188.

Esteban, M., Giner, J., 1980. Messinian coral reefs and erosion surfaces in Cabo de Gata (Almeria, S.E. Spain). Acta Geol. Hisp. 15, 97–104.

Flecker, R., Ducassou, E., Williams, T., Amarathunga, U., Balestra, B., Berke, M.A., Blättler, C.L., Chin, S., Das, M., Egawa, K., Fabregas, N., Feakins, S.J., George, S.C., Hernández-Molina, F.J., Krijgsman, W., Li, Z., Liu, J., Noto, D., Raad, F., Rodríguez-Tovar, F.J., Sierro, F.J., Standring, P., Stine, J., Tanaka, E., Teixeira, M., Xu, X., Yin, S., Yousfi, M.Z., 2025. Site U1611. In: Flecker, R., Ducassou, E., Williams, T. (Eds.), The Expedition 401 Scientists, Mediterranean–Atlantic Gateway Exchange. Proceedings of the International Ocean Discovery Program, 401. International Ocean Discovery Program, College Station, TX. https://doi.org/10.14379/iodp.proc.401.106.2025.

Föllmi, K.B., Hofmann, H., Chiaradia, M., de Kaenel, E., Frijia, G., Parente, M., 2015. Miocene phosphate-rich sediments in Salento (southern Italy). Sediment. Geol. 327, 55–71.
Franseen, E.K., Goldstein, R.H., 1996. Paleoslope, sea-level and climate controls on Upper Miocene platform evolution, Las Negras area, southeastern Spain. In: Franseen, E.K., Esteban, M., Ward, W.C., Rouchy, J.M. (Eds.), Models for Carbonate Stratigraphy from Miocene Reef Complexes of Mediterranean Regions, 5. SEPM, Concepts in Sedimentologytology and Paleontologyogy, pp. 159–176.
Franseen, E.K., Mankiewicz, C., 1991. Depositional sequences and correlation of middle (?) to late Miocene carbonate complexes, Las Negras and Níjar areas, southeastern Spain. Sedimentology 38, 871–898.
Franseen, E.K., Goldstein, R.H., Whitesell, T.E., 1993. Sequence stratigraphy of Miocene carbonate complexes, Las Negras area, southeastern Spain. Implications for quantification of changes in relative sea level. In: Loucks, R.G., Sarg, J.F. (Eds.), Carbonate Sequence Stratigraphy: Recent Developments and Applications, 57. AAPG Mem., pp. 409–434
Franseen, E.K., Goldstein, R.H., Farr, M., 1997. Substrate-slope and temperature controls on carbonate ramps: revelations from Upper Miocene outcrops, SE Spain. In: James, N.P., Clarke, J.A.D. (Eds.), Cool-water Carbonates, 56. SEPM Spec. Publ, pp. 271–292.
Franseen, E.K., Goldstein, R.H., Farr, M.R., 1998. Quantitative controls on location and architecture of carbonate depositional sequences; upper Miocene, Cabo de Gata region, SE Spain. J. Sediment. Res. 68 (2), 283–298.
Garcia, F., Conesa, G., Münch, P., Cornée, J.J., Saint Martin, J.P., André, J.P., 2004. Evolution des environnements littoraux du bassin de Melilla-Nador (Nord-Est Maroc) au Messinien superieur entre 6, 0 et 5, 77 Ma. Geobios 37 (1), 23–36.
Garcia-Castellanos, D., Heida, H., Palcu, D.V., Bulian, F., Sierro, F., 2025. Kilometric Sea level changes during the Messinian salinity crisis caused by river erosion and climate. Sci. Adv. 11 (28), eads9752.
Goldstein, R.H., Franseen, E.K., Lipinski, C.J., 2013. Topographic and sea level controls on oolite-microbialite-coralgal reef sequences: the terminal carbonate complex of Southeast Spain. AAPG Bull. 97 (11), 1997–2034.
Guiry, M.D., Guiry, G.M., 2025. AlgaeBase. World-wide Electronic Publication. National University of Ireland, Galway. https://www.algaebase.org.
Halfar, J., Godinez-Orta, L., Riegl, B., Valdez-Holguin, J.E., Borges, J.M., 2005. Living on the edge: high-latitude Porites carbonate production under temperate eutrophic conditions. Coral Reefs 24, 582–592.
Heida, H., Garcia-Castellanos, D., Jiménez-Munt, I., Estrada, F., Ercilla, G., Do Couto, D., Ammar, A., 2024. Seaway restriction, sea level drop and erosion in the Alboran Basin from a paleotopographic reconstruction for the Messinian Salinity Crisis. Mar. Geol. 474, 107300.
Hsü, K.J., 1972. Origin of saline giants: a critical review after the discovery of the Mediterranean evaporite. Earth Sci. Rev. 8, 371–396.
Hsü, K.J., Ryan, W.B.F., Cita, M.B., 1973. Late Miocene desiccation of the Mediterranean. Nature 242, 240–244.
Huang, W., Chen, J., Yang, E., Meng, L., Feng, Y., Chen, Y., Huang, Z., Tan, R., Xiao, Z., Zhou, Y., Xu, M., Yu, K., 2025. Heat-tolerant subtropical *Porites lutea* may be better adapted to future climate change than tropical one in the South China Sea. Sci. Total Environ. 962, 178381.
Krijgsman, W., Hilgen, F.J., Raffi, I., Sierro, F.J., Wilson, D.S., 1999. Chronology, causes and progression of the Messinian salinity crisis. Nature 400, 652–655.
Krijgsman, W., Fortuin, A.R., Hilgen, F.J., Sierro, F.J., 2001. Astrochronology for the Messinian Sorbas basin (SE Spain) and orbital (precessional) forcing for evaporite cyclicity. Sediment. Geol. 140 (1–2), 43–60.
Krijgsman, W., Capella, W., Simon, D., Hilgen, F.J., Kouwenhoven, T.J., Meijer, P.H., Sierro, F.J., Tulbure, M.A., van den Berg, B.C., van der Schee, M., Flecker, R., 2018. The Gibraltar Corridor: watergate of the Messinian Salinity Crisis. Mar. Geol. 403, 238–246.
Lipinski, C.J., Franseen, E.K., Goldstein, R.H., 2013. Reservoir analog model for oolite-microbialite sequences, Miocene terminal carbonate complex. Spain. AAPG Bull. 97 (11), 2035–2057.
Martín, J.M., Braga, J.C., 1994. Messinian events in the Sorbas Basin in southeastern Spain and their implications in the recent history of the Mediterranean. Sediment. Geol. 90 (3–4), 257–268.
Martín, J.M., Braga, J.C., Riding, R., 1993. Siliciclastic stromatolites and thrombolites, late Miocene, S.E. Spain. J. Sediment. Petrol. 63, 131–139.
Martín, J.M., Braga, J.C., Betzler, C., Brachert, T., 1996. Sedimentary model and high-frequency cyclicity in a Mediterranean, shallow-shelf, temperate-carbonate environment (uppermost Miocene, Agua Amarga Basin, Southern Spain). Sedimentology 43 (2), 263–277.
Martín, J.M., Braga, J.C., Riding, R., 1997. Late Miocene *Halimeda* alga-microbial segment reefs in the marginal Mediterranean Sorbas Basin, Spain. Sedimentology 44 (3), 441–456.
Martín, J.M., Braga, J.C., Betzler, C., 2003. Late Neogene–recent uplift of the Cabo de Gata volcanic province, Almería, SE Spain. Geomorphology 50 (1–3), 27–42.
Mas, G., Fornós, J.J., 2012. La Crisis de Salinidad del Messiniense en la cuenca sedimentaria de Palma (Mallorca, Islas Baleares). Geogaceta 52, 57–60.
Mather, A.E., 1991. Late Caenozoic Drainage Evolution of the Sorbas Basin, Southeast Spain. PhD thesis. University of Liverpool, p. 276.
Mather, A.E., Stokes, M., 2001. Marine to continental transition. In: A Field Guide to the Neogene Sedimentary Basins of the Almería Province, SE Spain, pp. 186–224.
Mattei, M., Riggs, N.R., Giordano, G., Guarnieri, L., Cifelli, F., Soriano, C.C., Jicha, B., Jasim, A., Marchionni, S., Franciosi, L., Tommasini, S., Porreca, M., Conticelli, S., 2014. Geochronology, geochemistry and geodynamics of the Cabo de Gata volcanic zone, Southeastern Spain. Ital. J. Geosci. 133 (3), 341–361.
Meilijson, A., Hilgen, F., Sepúlveda, J., Steinberg, J., Fairbank, V., Flecker, R., Waldmann, N.D., Spaulding, S.A., Bialik, O.M., Boudinot, F.G., Makovsky, Y., 2019. Chronology with a pinch of salt: integrated stratigraphy of Messinian evaporites in the deep Eastern Mediterranean reveals long-lasting halite deposition during Atlantic connectivity. Earth Sci. Rev. 194, 374–398.
Montenat, C., 1990. Les bassins néogènes du domaine bétique oriental (Espagne). Tectonique et sédimentation dan un couloir décrochant. Première partie: étude régionale, 12-13. Doc. et Trav. IGAL, Paris, p. 392.
Novak, V., Santodomingo, N., Rösler, A., Di Martino, E., Braga, J.C., Taylor, P.D., Johnson, K.G., Renema, W., 2013. Environmental reconstruction of a late Burdigalian (Miocene) patch reef in deltaic deposits (East Kalimantan, Indonesia). Palaeogeogr. Palaeoclimatol. Palaeoecol. 374, 110–122.
Padilla-Gamiño, J.L., Hanson, K.M., Stat, M., Gates, R.D., 2012. Phenotypic plasticity of the coral *Porites rus*: acclimatization responses to a turbid environment. J. Exp. Mar. Biol. Ecol. 434–435, 71–80.
Passaseo, C., Morsilli, M., 2024. Characterization of *Halimeda* bioherms of the pre-evaporitic Messinian of the Salento Peninsula (southern Italy). Sediment. Geol. 475, 106782.
Perrin, C., Bosellini, F.R., 2012. Paleobiogeography of scleractinian reef corals: changing patterns during the Oligocene–Miocene climatic transition in the Mediterranean. Earth Sci. Rev. 111, 1–24.
Perrin, C., Bosellini, F.R., 2013. The Late Miocene coldspot of z-coral diversity in the Mediterranean: patterns and causes. C. R. Palevol 12, 245–255.
Pomar, L., Ward, W.C., Green, D.G., 1996. Upper Miocene reef complex of the Llucmajor area, Mallorca, Spain. In: Models for Carbonate Stratigraphy from Miocene Reef Complexes of Mediterranean Regions, SEPM Concepts in Sedimentology and Paleontology, 5, pp. 191–225.
Reolid, J., Betzler, C., Braga, J.C., 2016. Amplitude of late Miocene Sea-level fluctuations from karst development in reef-slope deposits (SE Spain). Sediment. Geol. 345, 145–153.
Reuter, M., Bosellini, F.R., Budd, A.F., Coric, S., Piller, W., Harzhauser, M., 2019. High coral reef connectivity across the Indian Ocean is revealed 6-7 Ma ago by a turbid-water scleractinain assemblage from Tanzania (Eastern Africa). Coral Reefs 38, 1023–1037.
Riding, R., Braga, J.C., Martin, J.M., 1991a. Oolite stromatolites and thrombolites, Miocene, Spain: analogue of recent giant Bahamian examples. Sediment. Geol. 71, 121–127.
Riding, R., Martín, J.M., Braga, J.C., 1991b. Coral-stromatolite reef framework, upper Miocene, Almería, Spain. Sedimentology 38 (5), 799–818.
Riding, R., Awramik, S.M., Winsborough, B.M., Griffin, K.M., Dill, R.F., 1991c. Bahamian giant stromatolites: microbial composition of surface mats. Geol. Mag. 128, 227–234. https://doi.org/10.1017/S001675680002207X.
Riding, R., Braga, J.C., Martín, J.M., Sánchez-Almazo, I.M., 1998. Mediterranean Messinian Salinity Crisis: constraints from a coeval marginal basin, Sorbas, southeastern Spain. Mar. Geol. 146, 1–20.
Riding, R., Braga, J.C., Martín, J.M., 1999. Late Miocene Mediterranean desiccation: topography and significance of the `Salinity Crisis` erosion surface on-land in Southeast Spain. Sediment. Geol. 123, 1–7.
Rodríguez-Tovar, F.J., Sánchez-Almazo, I., Pardo-Igúzquiza, E., Braga, J.C., Martín, J.M., 2013. Incidence of obliquity and precession-forced Milankovitch cycles in the western Mediterranean: early Messinian sedimentation in the Sorbas Basin (Almería, southern Spain). Int. J. Earth Sci. 102 (6), 1735–1755.
Rosen, B.R., Aillud, G.S., Bosellini, F.R., Clack, N.J., Insalaco, E., Valldeperas, F.X., Wilson, M.E.J., 2002. Platy coral assemblages: 200 million years of functional stability in response to the limiting effects of light and turbidity. In: Proc. 9th Intern. Coral Reef Symp. Bali, pp. 255–264, 1.
Rouchy, J.M., Caruso, A., 2006. The Messinian salinity crisis in the Mediterranean basin: a reassessment of the data and an integrated scenario. Sediment. Geol. 188, 35–67.
Roveri, M., Gennari, R., Lugli, S., Manzi, V., 2009. The terminal carbonate complex: the record of sea-level changes during the Messinian salinity crisis. GeoActa 8, 63–77.
Roveri, M., Flecker, R., Krijgsman, W., Lofi, J., Lugli, S., Manzi, V., Sierro, F.J., Bertini, A., Camerlenghi, A., De Lange, G., Govers, R., Hilgen, F.J., Hübscher, Ch., Meijer, P., Stoica, M., 2014. The Messinian Salinity Crisis: past and future of a great challenge for marine sciences. Mar. Geol. 349, 113–125.
Roveri, M., Gennari, R., Persico, D., Rossi, F.P., Lugli, S., Manzi, V., Reghizzi, M., Taviani, M., 2019. A new chronostratigraphic and palaeoenvironmental framework for the end of the Messinian salinity crisis in the Sorbas Basin (Betic Cordillera, southern Spain). Geol. J. 54 (3), 1617–1637.
Roveri, M., Lugli, S., Manzi, V., 2025. The desiccation and catastrophic refilling of the Mediterranean: 50 years of facts, hypotheses, and myths around the Messinian salinity crisis. Annu. Rev. Mar. Sci. 17, 485–509.
Ruegg, G.J.H., 1964. Geologische onderzoekingen in het bekken van Sorbas, S Spanje, Geological Institute. University of Amsterdam, pp. 1–64.
Saint Martin, J.P., Conesa, G., Cornée, J.J., 1996. A new type of Messinian composite microbialitic build-up (Salemi, Sicily, Italy). Sediment. Geol. 106 (1–2), 51–63.
Saint Martin, J.P., André, J.P., Muller, J., Lapointe, P., 1997. Géométrie de la plate-forme carbonatée d'âge Messinien de Malte: mise en évidence de l'élévation du plan d'eau méditerranéen au cours du Messinien. Comptes rendus de l'Académie des sciences. Série 2. Sciences de la Terre et des planètes 324 (9), 729–736.
Saint-Martin, J.P., Néraudeau, D., Lauriat-Rage, A., Goubert, E., Secrétan, S., Babinot, J. F., Boukli-Hacene, S., Pouyet, S., Lacour, D., Pestrea, S., Conesa, G., 2000. La faune interstratifiée dans les gypses messiniens de Los Yesos (bassin de Sorbas, SE Espagne): implications. Geobios 33, 637–649.
Samperiz, A., Sosdian, S., Hendy, E., Johnson, K., John, E.H., Jupiter, S.D., Albert, S., 2025. Coastal seawater turbidity and thermal stress control growth of reef-building *Porites* spp. corals in Fiji. Sci. Rep. 15, 17172.

Sánchez-Almazo, I.M., 1999. Evolución paleoambiental de las cuencas neógenas de Almería en el Messiniense. Doctoral dissertation. Universidad de Granada.
Sánchez-Almazo, I.M., Spiro, B., Braga, J.C., Martín, J.M., 2001. Constraints of stable isotope signatures on the depositional palaeoenvironments of upper Miocene reef and temperate carbonates in the Sorbas Basin, SE Spain. Palaeogeogr. Palaeoclimatol. Palaeoecol. 175 (1–4), 153–172.
Sanchez-Almazo, I.M., Braga, J.C., Dinarés-Turell, J., Martín, J.M., Spiro, B., 2007. Palaeoceanographic controls on reef deposition: the Messinian Cariatiz reef (Sorbas Basin, Almería, SE Spain). Sedimentology 54 (3), 637–660.
Santodomingo, N., Novak, V., Pretkovic, V., Marshall, N., Di Martino, E., Lo Giudice Capelli, E., Rösler, A., Reich, S., Braga, J.C., Renema, W., Johnson, K.G., 2015. A diverse patch reef from turbid habitats in the Middle Miocene (East Kalimantan, Indonesia). Palaios 30, 128–149.
Sierro, F.J., Flores, J.A., Civis, J., Gonza, J.A., France, G., 1993. Late Miocene globorotaliid event-stratigraphy and biogeography in the NE-Atlantic and Mediterranean. Mar. Micropaleontol. 21 (1–3), 143–167.
Sierro, F.J., Hilgen, F.J., Krijgsman, W., Flores, J.A., 2001. The Abad composite (SE Spain): a Messinian reference section for the Mediterranean and the APTS. Palaeogeogr. Palaeoclimatol. Palaeoecol. 168 (1–2), 141–169.
Stafford-Smith, M.G., 1993. Sediment-rejection efficiency of 22 species of Australian scleractinian corals. Mar. Biol. 115 (2), 229–243.
Stokes, M., Mather, A.E., Rodés, Á., Kearsey, S.H., Lewin, S., 2018. Anatomy, age and origin of an intramontane top basin surface (Sorbas Basin, Betic Cordillera, SE Spain). Quaternary 1 (2), 15.
Vertino, A., Stolarski, J., Bosellini, F.R., Taviani, M., 2014. Mediterranean corals through time: From miocene to present. In: Goffredo, S., Dubinsky, Z. (Eds.), The Mediterranean Sea: Its History and Present Challenges. Springer, pp. 257–274.
Vescogni, A., Bosellini, F.R., Reuter, M., Brachert, T.C., 2008. Vermetid reefs and their use as palaeobathymetric markers: new insights from the Late Miocene of the Mediterranean (Southern Italy, Crete). Palaeogeogr. Palaeoclimatol. Palaeoecol. 267, 89–101.
Vescogni, A., Guido, A., Mastandrea, A., Russo, F., 2011. Microbialite-vermetid community (Salento Peninsula, southern Italy): a late Miocene example of automicrite deposition. In: Reitner, J., Quéric, N.V., Arp, G. (Eds.), Advances in Stromatolite Geobiology, 131. Lect. Notes Earth Sci., pp. 321–329
Vescogni, A., Vertino, A., Bosellini, F.R., Harzhauser, M., Mandic, O., 2018. New paleoenvironmental insights on the Miocene condensed phosphatic layer of Salento (southern Italy) unlocked by the coral-mollusc fossil archive. Facies 64, 7.
Vescogni, A., Guido, A., Cipriani, A., Gennari, R., Lugli, F., Lugli, S., Manzi, V., Reghizzi, M., Roveri, M., 2022. Palaeoenvironmental setting and depositional model of upper Messinian microbialites of the Salento Peninsula (Southern Italy): a Central Mediterranean Terminal Carbonate complex. Palaeogeogr. Palaeoclimatol. Palaeoecol. 595, 110970.
Vescogni, A., Colombo, F., Guido, A., 2025. New insights into upper Messinian microbial carbonates: a dendrolite-thrombolite buildup from the Salento Peninsula, Central Mediterranean. Geobiology 23, e70023.